Flavour and Fragrance Journal

WILEY

ORIGINAL ARTICLE OPEN ACCESS

Integrated Anatomical, Chemical, Biological and Computational Studies Approach of *Myrcia sylvatica* (G. Mey) DC. A Multifaceted Insight Into a Promising Amazonian Species

Eliza de Jesus Barros dos Santos[1] | Zelina Ataíde Correia[1] | Ely Simone Cajueiro Gurgel[1] | Leonardo Souza da Costa[2] | Mabrouk Horchani[3] | Hayet Edziri[4] | Ravendra Kumar[5] | Anderson de Santana Botelho[2,6] | Karyme do Socorro de Souza Vilhena[7] | Eloisa Helena de Aguiar Andrade[1,2] | Mozaniel Santana de Oliveira[1,2]

[1]Graduate Program in Biological Sciences – Tropical Botany, Universidade Federal Rural da Amazônia and Museu Paraense Emílio Goeldi, Belém, Pará, Brazil | [2]Adolpho Ducke Laboratory – Botany Coordination, Museu Paraense Emílio Goeldi, Belém, PA, Brazil | [3]Laboratory of Heterocyclic Chemistry, Natural Products and Reactivity, Medicinal Chemistry and Natural Products (LR11ES39), Faculty of Sciences of Monastir, University of Monastir, Monastir, Tunisia | [4]Laboratory of Transmissible Diseases and Biologically Active Substances, Faculty of Pharmacy, 5000, University of Monastir, Monastir, Tunisia | [5]Department of Chemistry, College of Basic Sciences and Humanities, G.B. Pant University of Agriculture and Technology, Pantnagar, Uttarakhand, India | [6]Graduate Program in Chemistry, Federal University of Pará, Belém, Pará, Brazil | [7]Faculty of Chemistry, Institute of Exact and Natural Sciences, Federal University of Pará, Belém, Pará, Brazil

Correspondence: Mozaniel Santana de Oliveira (mozaniel.oliveira@yahoo.com.br)

Received: 4 June 2025 | **Revised:** 6 November 2025 | **Accepted:** 18 November 2025

Keywords: antioxidant activity | essential oils | molecular docking | *Myrcia sylvatica* | sesquiterpenes

ABSTRACT

Myrcia sylvatica (G. Mey) DC, a native aromatic species from the Brazilian Amazon, was comprehensively studied for its anatomical, histochemical, chemical and biological characteristics, including an in silico evaluation. Leaves were subjected to anatomical and histochemical analysis, revealing secretory structures associated with the accumulation of lipids, terpenes, alkaloids and phenolic compounds. Essential oils were extracted by hydrodistillation (HD) and steam distillation (SD) and chemically characterised via GC–MS, revealing sesquiterpenes such as α-zingiberene, germacrene D and spathulenol as major constituents. The SD-extracted oil presented higher antioxidant activity (ABTS IC_{50} = 6.80 mg/mL; DPPH IC_{50} = 12.80 mg/mL) and greater toxicity against *Artemia salina* (LC_{50} = 4.17 μg/mL) than the HD essential oil. Correlation analysis indicated distinct biosynthetic clusters of compounds. Molecular docking and ADME analysis highlighted spathulenol and globulol as promising bioactive molecules with potential acetylcholinesterase inhibitory activity and favourable pharmacokinetic profiles. These results provide unprecedented insights into the bioactive potential and chemical ecology of *M. sylvatica*, supporting its application in natural product development.

1 | Introduction

The Myrtaceae has a great diversity of species, with around 142 genera and 6000 species distributed throughout tropical and subtropical regions. In Brazil, the family has a remarkable number of native and endemic species, with confirmed occurrences in the north, northeast, midwest, southeast and south [1, 2]. Myrtaceae plays a significant role in traditional medicine due to the bioactive potential of many of its species [3].

Amongst the species of the Myrtaceae, the *Myrcia* genus stands out due to its therapeutic properties, as it produces a large

This is an open access article under the terms of the Creative Commons Attribution License, which permits use, distribution and reproduction in any medium, provided the original work is properly cited.

© 2025 The Author(s). *Flavour and Fragrance Journal* published by John Wiley & Sons Ltd.

amount of essential oil in its secondary metabolism, rich in compounds such as monoterpene, sesquiterpene and phenolic compounds, making the genus have great biological potential, such as antimicrobial, phytotoxic, antioxidant, insecticide and hypoglycemic, amongst others [4, 5].

Within this context, *Myrcia sylvatica* (G. Mey) DC, popularly known as 'Pedra-ume-caá,' stands out for its chemical and biological properties. Studies indicate that *M. sylvatica* produces essential oils with variations in chemical composition influenced by extrinsic factors, such as environmental conditions [6]. Several studies have been conducted to investigate the chemical composition and biological properties of *M. sylvatica* [6–10].

Research has identified the main compounds present in the plants' essential oil, including hydrocarbon and oxygenated sesquiterpenes and phenolic compounds [6–10]. These compounds have been associated with antioxidant, anti-inflammatory and toxicity activities [9–11], which may be useful in the treatment of various diseases.

However, there are gaps in the literature on the anatomical and histochemical aspects and biological properties of *M. sylvatica*. Filling these gaps is important because a detailed understanding of the anatomy and histochemistry of the species can provide information on the production and storage sites of the metabolites that the species presents. In addition, the chemical characterisation of the essential oil of *M. sylvatica* is fundamental to understanding its chemical variability, which can contribute to the development of new natural products with medicinal applications.

The aim of this study was to characterise the chemical composition of the essential oil of *M. sylvatica*, to provide unpublished information on its anatomical and histochemical characteristics, and to evaluate its antioxidant potential, toxicity and *in silico* study, thus contributing to knowledge of the species' biological potential.

2 | Material and Methods

2.1 | Sample Collection and Processing

M. sylvatica leaves were collected in the environmental preservation area of the Utinga State Park, located in Belém, Pará, Brazil (Figure 1). This site was chosen due to its representativeness of floodplain and terra firme forest ecosystems, typical of the Amazon, where the species is native. In addition, the park offers a protected and monitored area, which guarantees the integrity of the botanical material collected.

The species was collected following the protocols for field collection and herborisation. The exsiccate, botanical

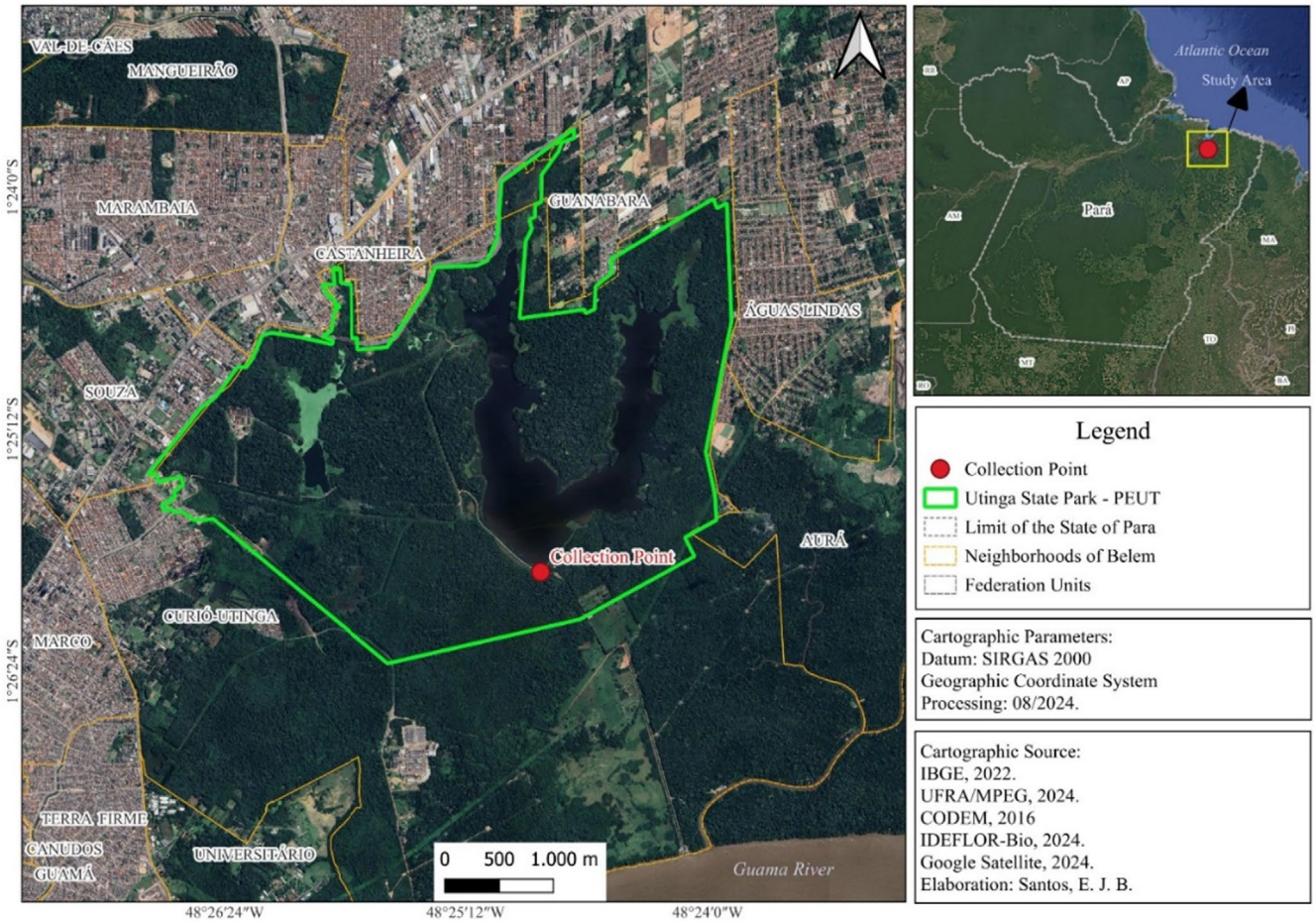


FIGURE 1 | Map illustrating the collection site in Utinga State Park (PEUT).

identification and registration of the species were deposited in the João Murça Pires Herbarium of the Museu Paraense Emílio Goeldi, Belém, Pará, with the following registration number MG254169, the species is also registered in SisGen A965505.

2.2 | Anatomical Analysis of the Leaf Blade by Light Microscopy (LM)

Parts of the leaf blade of *M. sylvatica* in natura, including the median region, central vein, margin and petiole, as shown in Figure 2, were fixed in formaldehyde, acetic acid and 50% ethanol (FAA) [12] for 24 h for structural analysis. For the histochemical tests, the samples were fixed in FAA to check for hydrophilic substances, neutral buffered formalin (NTF) to check for lipophilic substances and ferrous sulphate in formalin (SFF) to determine total phenolic compounds [12, 13].

The samples were then dehydrated in an increasing series of tertiary butyl alcohol for inclusion in histological paraffin with dimethyl sulfoxide (DMSO) (Paraplast, Leica Biosystems, Teaneck, NJ, USA) [12]. Transverse and longitudinal sections of 11 μm were obtained using a rotary microtome (Leica model RM 2245, Leica Biosystems, Heidelberg, Germany). Part of the samples was stained with astra blue and safranin [14], while the rest was used for histochemical tests. The slides were mounted in colourless Canada balsam [15].

2.3 | Dissociation of the Epidermis

To dissociate the epidermis, fractions of leaves were sectioned with a steel blade and immersed in a solution of hydrogen peroxide and acetic acid for 24 h [16]. After this period, the samples were washed in distilled water and stained with safranin [14]. Subsequently, the slides were mounted in aqueous glycerin (1:1), with the edges duly sealed using colourless enamel, as described by Purvis et al. [17].

2.4 | Histochemistry

In the analysis of the metabolic groups present in the samples, different reagents were used to identify and characterise the compounds. For the detection of total lipids, the Sudan Black reagent was used, as described by Pearse [18]. Acid lipids were identified using Nile blue sulphate, following the methodology of Cain [19]. Terpenes were visualised using the Nadi reagent, which followed the protocol described by David and Carde [20].

The presence of phenolic compounds was determined using the (SFF) reagent, as described by Johansen [12], while tannins were detected using hydrochloric vanillin solution, following the method described by Mace and Howell [21].

Lignin was analysed using the phloroglucinol reagent, following the studies of Johansen [12]. For the detection of acid mucilage, the ruthenium red reagent was used, following the studies of Gregory and Baas [22]. Total polysaccharides were detected using the PAS reagent (Periodic Acid Schiff's reagent), according to the studies of McManus [23], and for the identification of starch, the lugol reagent was used, following the methodology of Johansen [12]. Alkaloids were detected using the Wagner reagent, based on the studies of Furr and Mahlberg [24], and the presence of crystals was detected using 5% hydrochloric acid, as described in the studies of Chamberlain [25].

Photographic records of both anatomy and histochemistry were taken on a Leica microscope (DM6B, Wetzlar, Germany) coupled to a digital camera (Leica application suite LAS V4.12) in the

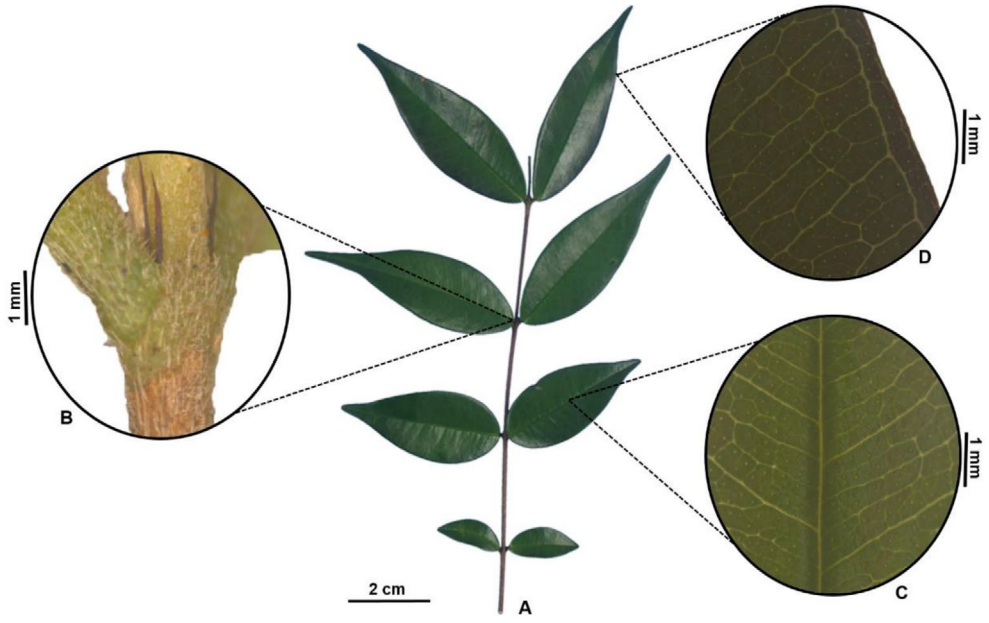


FIGURE 2 | Leaf structure of *Myrcia sylvatica* (G. Mey) DC. (A) General view of the branch, (B) Petiole (C) Median region and central vein, (D) Margin.

Botany Microscopy Laboratory at the Museu Paraense Emílio Goeldi (MPEG), calibrated with suitable micrometre slides as specified by the manufacturer.

2.5 | Extraction Methods

The *M. sylvatica* leaves were dried in an air-conditioned room with temperature and humidity control using air conditioning and a dehumidifier. The material was ground in a knife mill.

For the essential oil extraction process, the dried leaves were subjected to two distillation methods: steam (SD) and hydrodistillation (HD). Both methods used a modified Clevenger-type glass system with an extraction time of 3 h. The AV method used 1.666 kg of dried leaves, while the HD method used 1.415 kg of material, following the methods described by de Oliveira et al. [26].

The EOs were centrifuged for 5 min at 3000 rpm, dehydrated with anhydrous sodium sulphate (Na_2SO_4) and centrifuged again under the same conditions. They were then stored in amber glass ampoules and kept refrigerated at a constant temperature of −5°C. The percentage of water in the samples studied was determined using an infrared moisture analyser. The EO yield was calculated on a moisture-free basis using the ratio between mass, oil and moisture, as established by [27].

2.6 | Identification of Chemical Components by GC/MS

The chemical composition of the EOs was analysed by gas chromatography coupled to mass spectrometry (GC/MS) on a SHIMADZU QP Plus-2010 system equipped with a DB-5MS silica capillary column (30 m × 0.25 mm; film thickness 0.25 μm) under the following operating conditions: carrier gas: helium, linear velocity 36.5 cm s^{-1}; injection mode: splitless (2 μL of oil in 0.5 mL of hexane); injector temperature: 250°C, temperature programme: 60°C–250°C with a gradient of 3°C min^{-1}; the temperature of the ion source for other parts was kept at 220°C. The scan time of the quadrupole was 39 to 500 Da s^{-1}. Ionisation was carried out in electron impact mode at 70 eV. Identification of the volatile components was based on the linear retention index (RI) and the mass spectral fragmentation pattern, comparing the data with authentic samples from the Adams library [28]. The RIs were obtained using the homologous series of n -alkanes (C_8–C_{40}) from Sigma-Aldrich (San Luis, AZ, USA).

2.7 | Preliminary Toxicity Bioassay With Artemia

For the toxicity tests, the essential oil of *M. sylvatica* obtained by HD and AV was evaluated in relation to the larvae of the microcrustacean *Artemia salina*, as described in the literature [26, 29]. The *A. salina* eggs were incubated at room temperature (27°C–30°C) in an aquarium containing artificial salt water made up of a mixture of 46 g of NaCl, 22 g of $MgCl_2$.$6H_2O$, 8 g of Na_2SO_4, 2.6 g of $CaCl_2$.$6H_2O$, 1.4 g of KCl in 2.0 L of distilled water. The pH was adjusted to between 8.0 and 9.0 using Na_2CO_3. Twenty-four hours after the eggs hatched, oil solutions were prepared at concentrations of 100, 50, 25, 10, 5 and 1 μg/mL, using brine water and 5% DMSO as a diluent. In each tube containing the solutions, 10 *A. salina* larvae were added and, after 24 h, the mortality rate of the larvae was calculated, estimating the average lethal concentration (LC_{50}), using the Probits statistical method.

2.8 | Testing the Antioxidant Capacity of Essential Oils

2.8.1 | $ABTS^{\bullet+}$ Test

The radical inhibition activity (RIA) of the diammonium salt 2,2′-azino-bis (3-ethylbenzothiazoline-6-sulfonic acid) ($ABTS^{-+}$) was analysed according to the study by Kuskoski et al. [30], with modifications. Initially, ABTS (7 mM L^{-1}) and potassium persulphate (140 mM L^{-1}) were mixed and left in the dark for 16 h to form the $ABTS^{\bullet+}$ radical (2.45 mM L^{-1}). The radical was then diluted in phosphate-buffered saline until it reached an absorbance of 0.700 ± 0.05 in a Genesys50 spectrophotometer (Thermo Scientific) at 734 nm. Next, 30 μL of samples at concentrations of 4, 8, 12, 16 and 20 mg/mL of the HD and AV oils prepared in ethanol or the positive control (Trolox) at concentrations of 2, 4, 6, 8 and 10 μg/mL were added to 2 mL of the $ABTS^{\bullet+}$ solution. The absorbance was read after 6 min of reaction at 743 nm. This procedure was carried out in duplicate and ethanol was used as a negative control. RIA was calculated according to the equation:

$$\text{RIA}\,(\%) = \frac{\left(A_{\text{control}} - A_{\text{sample}}\right)}{A_{\text{control}} \times 100} \tag{2}$$

where A_{control} represents the absorbance of the $ABTS^{-+}$radical (2.5 mM L^{-1}), A_{sample} the absorbance of the sample and A_{control} the absorbance of the negative control.

2.8.2 | $DPPH^{\bullet}$ Test

The RIA of 2,2-diphenyl-1-picrylhydrazyl ($DPPH^{\bullet}$) was determined according to the studies by Brand-Williams et al. [31], with modifications. Firstly, a solution of $DPPH^{\bullet}$ 60 μM L^{-1} was prepared in ethanol (PA; C_2H_6O; Sigma-Aldrich; 216224; São Paulo/SP, Brazil). The absorbance of the $DPPH^{\bullet}$ solution was then read on a Genesys50 spectrophotometer (Thermo Scientific) at 517 nm. Next, 50 μL of the samples at concentrations of 4, 8, 12, 16 and 20 mg/mL and the positive control (Trolox) at concentrations of 2, 4, 6, 8 and 10 μg/mL were added to 1.95 mL of the $DPPH^{\bullet}$ solution and stored away from light for 1 h. The test was carried out in duplicate and ethanol was used as a negative control. The calculation was carried out according to Equation (2).

The antioxidant activity data was processed and presented as mean ± standard deviation, inhibitory concentration (IC_{50}) and trolox equivalent antioxidant capacity (TEAC). The IC_{50}values of the samples and trolox were calculated using non-linear regression analysis, respectively. The statistical treatment and graphs were carried out and generated using GraphPad Prism 10 software. Tukey's statistical test was also carried out where the statistical difference was considered significant when $p < 0.05$.

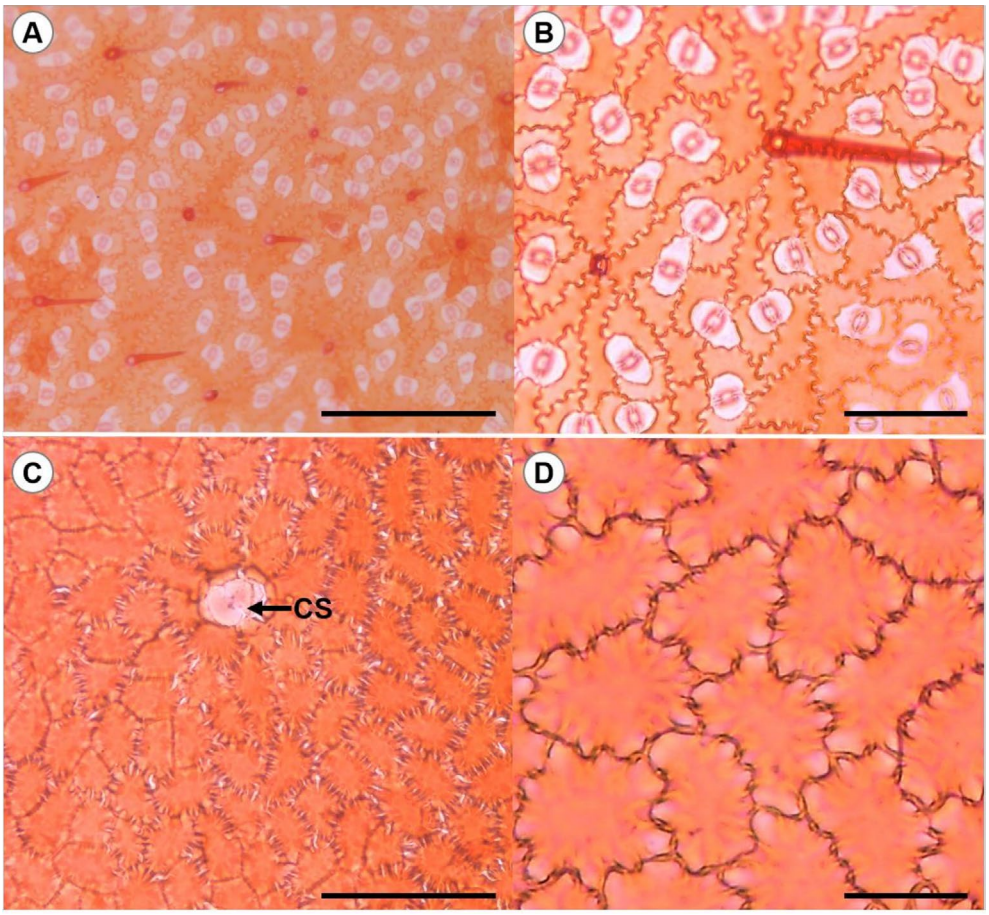


FIGURE 3 | Front view of the leaf of *Myrcia sylvatica* (G. Mey) DC. (A–D). (A) General view of the abaxial surface. (B) Paracytic stomata on the abaxial surface. (C) General view of the adaxial surface with secretory cavity (arrow). (D) Adaxial surface with detail of cells with sinuous anticlinal walls. Scale bar: 100 μm (B, D), 200 μm (A, C).

2.9 | Statistical Analysis

Correlations amongst the chemical compounds were evaluated using Pearson's linear correlation, considering only compounds with a minimum concentration of 0.5 in at least one of the analysed samples. The aim was to identify patterns of direct or inverse association amongst the metabolites present in the samples. The correlation matrix was constructed based on the quantitative values of the relative concentrations of the compounds, allowing the identification of groups of substances with similar or antagonistic chemical behaviour. Analyses were performed using Minitab version 22 (free version, Minitab LLC), and the results were presented as a correlogram, in which the intensity and direction of the correlations are represented by a bidirectional colour scale.

2.10 | Materials and Methods

2.10.1 | Molecular Docking Procedure

Molecular docking simulations were carried out by the Auto Dock 4.2 program package [32]. The X-ray crystal structure of AChE complexed with 'donepezil' was sourced from Protein Data Bank (PDB code: 1EVE) [33]. The water molecules (H_2O) in the protein's structure were removed and the steps were done: add the missing hydrogens in addition to assigning the partial charges (Gasteiger). The AutoDock Tools were used to prepare the ligands and protein files (PDBQT). The optimisation of all the geometries of ligands was conducted by using ACD (3D viewer) software (http://www.filefacts.com/acd3d-viewer-freeware-info) and the visualisation and analysis of interactions were carried out via Discovery Studio 2017R2 (https://www.3dsbiovia.com/products/collaborative-science/biovia-discovery-studio/).

2.10.2 | ADME Properties

The pharmacokinetic and drug-likeness properties of the main phytocompounds were estimated by using ADME (absorption, distribution, metabolism and excretion) descriptors via a SwissADME online server (http://www.swissadme.ch/).

3 | Results and Discussion

3.1 | Anatomical Characterisation

As a result of the anatomical characterisation of *M. sylvatica*, it was observed that, in frontal view, the epidermis on both sides consists of cells with sinuous anticlinal walls (Figure 3A–D). In cross section, it was observed that the mesophyll epidermis is

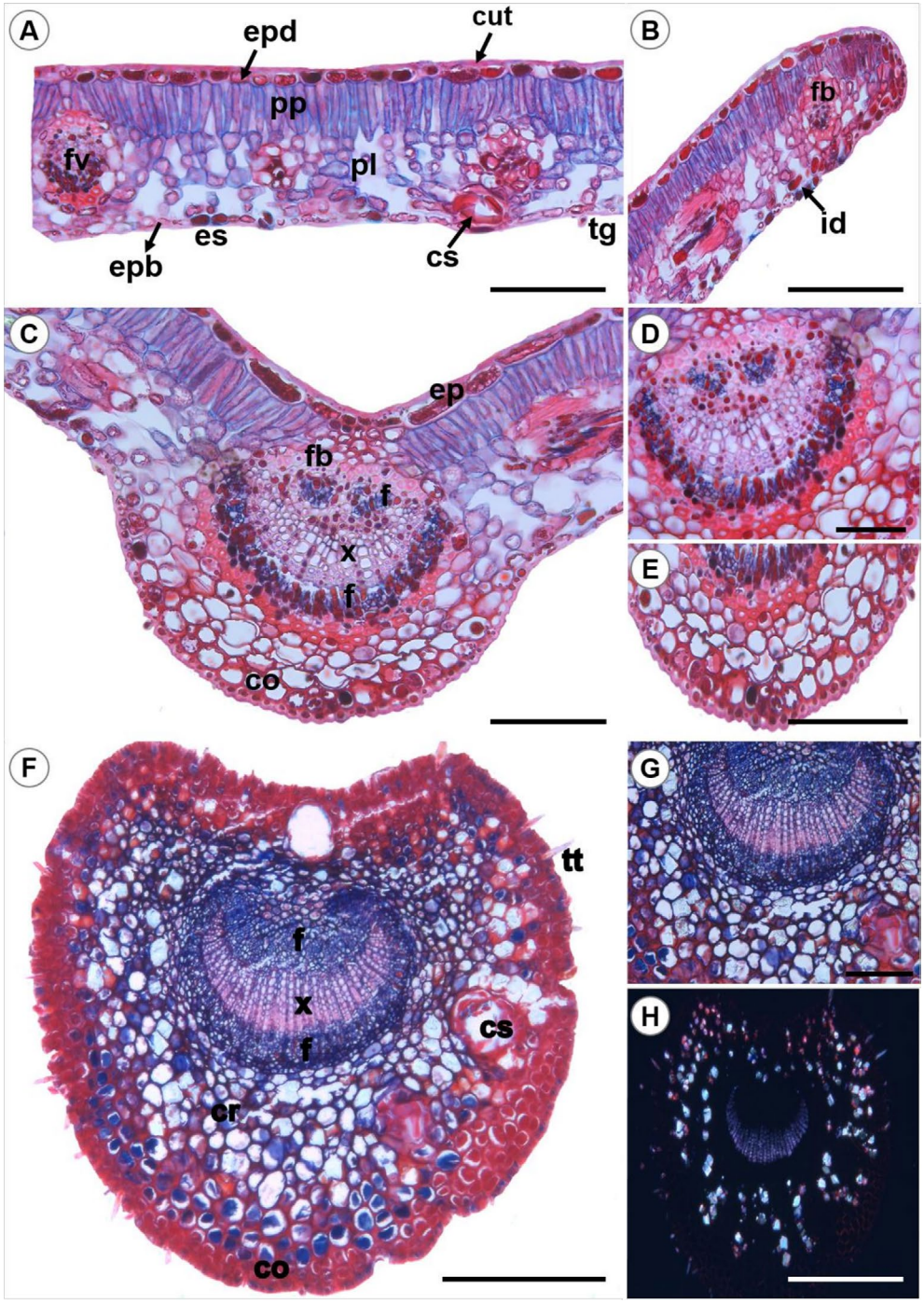


FIGURE 4 | Transverse section of the leaf of *Myrcia sylvatica* (G. Mey) DC. (A) General view of the mesophyll, (B) Margin, (C) General view of the central vein. (D) Detail of the vascular bundle. (E) Detail of the epidermis and collenchyma. (F) General view of the petiole. (G) Detail of the vascular bundle. (H) General view of the petiole under polarised light. co, colenchyma; cr, crystals; cs, secretory cavity; cut, cuticle; ep, epidermis; epb, abaxial epidermis; epd, adaxial epidermis; es, stomata; f, phloem; fb, sclerenchymatous fibre; fv, vascular bundle; id, secretory idioblast; tg, glandular trichome; tt, tectores trichome. Scale bar: 50 μm (D, G), 100 μm (A, B, C, E, H), 200 μm (F).

unistratified, consisting of tabular cells, and the margin has the same epidermal characteristics as the mesophyll (Figure 4A,B). The epidermal cells present in the adaxial part of the central vein of *M. sylvatica* are large and tabular, while in the abaxial phase the cells are rounded and small (Figure 4C,E).

The epidermis is covered by a thick, smooth cuticle (Figure 4A–C,F). The stomata are located at the same level as the other epidermal cells and are anomocytic, with a hypoestomatic arrangement (Figures 3A,B and 4). In addition, the epidermis contains unicellular trichomes with sharp apices (Figures 3 and 4) and unicellular and multicellular glandular trichomes (Figure 4A,F).

These anatomical structures are characteristic of *Myrcia* DC. species, reflecting their ability to adapt to different environments.

For example, the hypostome minimises water loss from the plant, while the paracytic stomata have subsidiary cells aligned parallel to guard cells, allowing greater control over the opening and closing of stomatal pores and enabling water homeostasis. Another adaptation observed in *M. sylvatica* is the sinuous anticlinal walls that contribute to the flexibility and support of the epidermis [34, 35].

The mesophyll of *M. sylvatica* is dorsiventral, presenting palisade parenchyma with two layers of cells and lacunar parenchyma with 5 to 6 layers of cells. In addition, secretory idioblasts, prismatic crystals and secretory cavities are found in the lacunar parenchyma (Figure 4A). The secretory cavities were located in the palisade and lacunar parenchyma and consisted of a single-layered secretory epithelium of thin-walled tabular cells delimiting the lumen (Figure 4A). These characteristic anatomical structures are associated with the production, storage and secretion of bioactive compounds and are found in some species of the genus *Myrcia* [34, 35]. This dorsiventral organisation of the mesophyll aids in the absorption of light and the circulation of oxygen and carbon dioxide, which are essential for maximising the efficiency of photosynthesis in high-light environments. This characteristic aids in the classification and taxonomic identification within the Myrtaceae family [35, 36].

The margin has a structure similar to the midrib, but the mesophyll region has rounded cells with the same characteristics as the mesophyll. However, the cells of the palisade and spongy parenchyma are more compact (Figure 4B). In the lacunar parenchyma, there are collateral vascular bundles surrounded by sclerenchymatic fibres. These fibres help filter light in the inner layers of the mesophyll during photosynthesis [37].

The midrib has a flat convex shape (Figure 4C). The flat convex shape of the midrib of *M. sylvatica* is a characteristic that can vary amongst species of the genus, and this variation reflects the morphological diversity of *Myrcia*, reinforcing the phenotypic plasticity and adaptive capacity of the genus [38, 39].

The cortex of the rib is formed by 1–2 layers of angular collenchyma (Figure 4C,E). The parenchymatic tissue is formed by polygonal cells with spaced walls and intracellular spaces containing numerous secretory idioblasts. The vascular system is organised into a bicolateral vascular bundle surrounded by a sheath of sclerenchymatic fibres (Figure 4D). The vascular system, organised into a bicolateral bundle, is a characteristic commonly found in the genus *Myrcia* [38, 39].

The petiole in cross section is flat and convex with a single-layered epidermis consisting of rectangular cells with glandular trichomes and tectorial trichomes. It is also covered by a smooth, spaced cuticle (Figure 4F). In the cortex, there are 2–3 layers of lamellar collenchyma, and the parenchymatic tissue is formed by polygonal, heterodimeric cells with thick walls (Figure 4F). In the parenchymatic tissue, there are secretoid idioblasts, secretory cavities, and prismatic crystals (Figure 4F–H). The vascular bundle is bicolateral (Figure 4F–H). The petiole and midrib of the species under study differ from other species of the genus in terms of the shape and organisation of the vascular system [34, 39, 40].

3.2 | Histochemistry

Histochemical tests performed on *M. sylvatica* leaves reacted to different metabolic classes, testing positive in idioblasts, secretory cavities, secretory epidermis, and glandular trichomes. These structures store and secrete bioactive metabolites, which perform functions related to growth, protection, and defence against pathogens and herbivores [34, 41, 42]. The results of the histochemistry are shown in Table 1, and the reactions are shown in Figures 5 and 6.

The positive reaction of total lipids, acid lipids, terpenes, and phenolic compounds in specialised structures such as idioblasts, secretory cavities, secretory epidermis, and glandular trichomes. The identification of the secretory epidermis in *M. sylvatica* is heterogeneous, which is an unprecedented characteristic for the genus *Myrcia*. The positive reaction of these bioactive compounds in these specialised structures indicates that these compounds play important roles in defence and metabolism regulation, contributing to the growth and development of *M. sylvatica* [5, 40, 43–46].

Lipophilic compounds such as total lipids, acid lipids and terpenes are metabolites found in species of the Myrtaceae family [40, 45, 46]. These compounds play important roles, especially in defence against biotic and abiotic factors [44]. Species of the *Myrcia* genus are known for producing volatile compounds in their secondary metabolism, such as essential oil, which has terpenes as its main constituents. Terpenes play an important role in the ecosystem, as they act in defence against herbivores and pathogens, and also have antimicrobial, phytotoxic, antioxidant and hypoglycemic activities, amongst others [5, 43].

Histochemical tests also demonstrated the presence of phenolic compounds in the idioblasts, secretory cavities, secretory epidermis, and glandular trichomes of *M. sylvatica*. The presence of phenolic compounds indicates the therapeutic potential of this species, especially in the prevention of diseases related to oxidative stress [7, 43, 47]. This data corresponds with the metabolic profile of other species of the *Myrcia* genus, which are known for the presence of phenolic compounds [5, 43].

The tests qualitatively show that *M. sylvatica* presented acid mucilage, alkaloids, and total polysaccharides in the idioblasts, secretory cavities, secretory epidermis, and glandular trichomes. Acid mucilage aids in water retention and protection against environmental stresses [48]. Alkaloids are important for protection against herbivores and are known for their antimicrobial and anticancer properties [49, 50]. Total polysaccharides have immunomodulatory properties, that is, they are able to regulate the immune system's response [51], and have anti-inflammatory potential [52].

The positive result for hydrochloric vanillin indicated the presence of tannins in the idioblasts of *M. sylvatica*. Souza-Moreira et al. [53], observed that the polar extracts of *Plinia. cauliflora* (Myrtaceae), rich in tannins, showed activity against Candida species. This corroborates the literature reports on the antifungal potential of species from the Myrtaceae family [54–56]. Idioblasts have also been shown to contain calcium oxalate crystals, which are commonly found in the leaves of species from the

TABLE 1 | Results of the histochemical tests on the leaf lamina and petiole of *Myrcia sylvatica* (G. Mey) DC.

		Structures				
Reagent	**Metabolites**	**Idioblast**	**Secretory cavities**	**Secretory epidermis**	**Secretory trichomes**	**Other structures**
Sudan Black	Total lipids	+	+	+	+	−
Nile blue sulphate	Acid lipids	+	+	+	+	−
Nadi's reagent	Terpenes	+	+	+	+	−
SFF (iron sulphate in formalin)	Phenolic compounds	+	+	+	+	−
Hydrochloric vanillin	Tannin	+	−	−	−	−
Floroglucinol	Lignin	−	−	−	−	+
Ruthenium red	Acid mucilage	+	+	+	+	−
PAS (Periodic Acid Schiff's reagent)	Total polysaccharides	+	+	+	+	−
Lugol's reagent	Starch	−	−	−	−	+
Wagner	Alkaloid	+	+	+	+	−
Hydrochloric acid 5%	Crystals of Calcium oxalate	+	−	−	−	−

Note: (+) positive reaction, (−) negative reaction.

Myrtaceae family, such as *Eucalyptus saligna* Sm, [57], *Myrcia hatschbachii* D. Legrand [34], *Myrcia multiflora* (Lam.) DC, [39], *Plinia cauliflora* (DC.) Kausel [53].

Although *M. sylvatica* has several secretory structures, starch and lignin were detected in the xylem and palisade parenchyma. Lignin and starch are two essential substances for plant physiology and development, providing functions such as maintaining cell structure, defence against pathogens and energy reserves [58, 59].

3.3 | Chemical Composition of the Essential Oil

In total, 57 constituents were identified in HD and 84 were identified in steam distillation, both quantified by gas chromatography coupled with mass spectrometry (GC/MS), as shown in Table 2. The yield of essential oil from the dried leaves of *M. sylvatica* obtained by steam distillation was 0.24%, while by hydrodistillation it was 0.41%. The difference in the yields of the essential oils may be related to the extraction technique used. Studies on other species have shown that both hydrodistillation (HD) and steam distillation (SD) influence the yield of essential oil [61, 62].

Figure 7 shows the two-dimensional structures of the constituents with the highest concentration identified in the essential oils of *M. sylvatica* from the SD and HD extraction techniques. With regard to the chemical profile of *M. sylvatica*, the essential oil obtained by SD was characterised as consisting mainly of sesquiterpene hydrocarbons (72.42%) and oxygenated sesquiterpenes (24.65%), while the essential oil obtained by HD also showed a predominance of sesquiterpene hydrocarbons (51.82%) and oxygenated sesquiterpenes (45.02%).

The α-zingiberene was identified at a concentration of 14.27% in the essential oil obtained by steam distillation, and 9.14% in the essential oil obtained by hydrodistillation, and the same compound was identified in the essential oil of other specimens of *M. sylvatica*, albeit in lower concentrations. In the studies by Silva et al. [63], α-zingiberene had a concentration of 0.2%, while in the studies by Sacool et al. [64] α-zingiberene had a concentration of 0.41%. The variation in the concentration of α-zingiberene shows the chemical variation of the species, which is caused by the influence of environmental and genetic factors.

In the studies by Costa et al. [6], the chemical characterisation of the essential oil of seven specimens of *M. sylvatica* was carried out, showing a chemical variability in the essential oil of the species, which was evidenced by the presence of four chemical profiles. These findings show that seasonality, collection site, genetics and plant part can contribute to variations in the chemical profile of *M. sylvatica*.

Essential oils containing high concentrations of α-zingiberene may have the potential to inhibit the production of aflatoxins and other fungal mycotoxins. Nerilo et al. [65] evaluated the efficacy of the essential oil of ginger (*Zingiber officinales* Roscoe), rich in α-zingiberene with a concentration of 23.85%, The study showed that the mycelial growth of *Aspergillus flavus* was reduced at a concentration of 150 $\mu g\,mL^{-1}$ of essential oil, and inhibition of the germination of conidia was shown at a concentration of 10 $\mu g\,mL^{-1}$. In addition, ergosterol biosynthesis was inhibited at a concentration of 10 and 15 $\mu g\,mL^{-1}$of essential oil was able to inhibit aflatoxin production by *A. flavus*.

Vasconcelos et al. [66], analysed the chemical composition of the essential oil of *M. vittoriana*, with germacrene D (21, 90%) being the main constituent. According to the authors, the essential

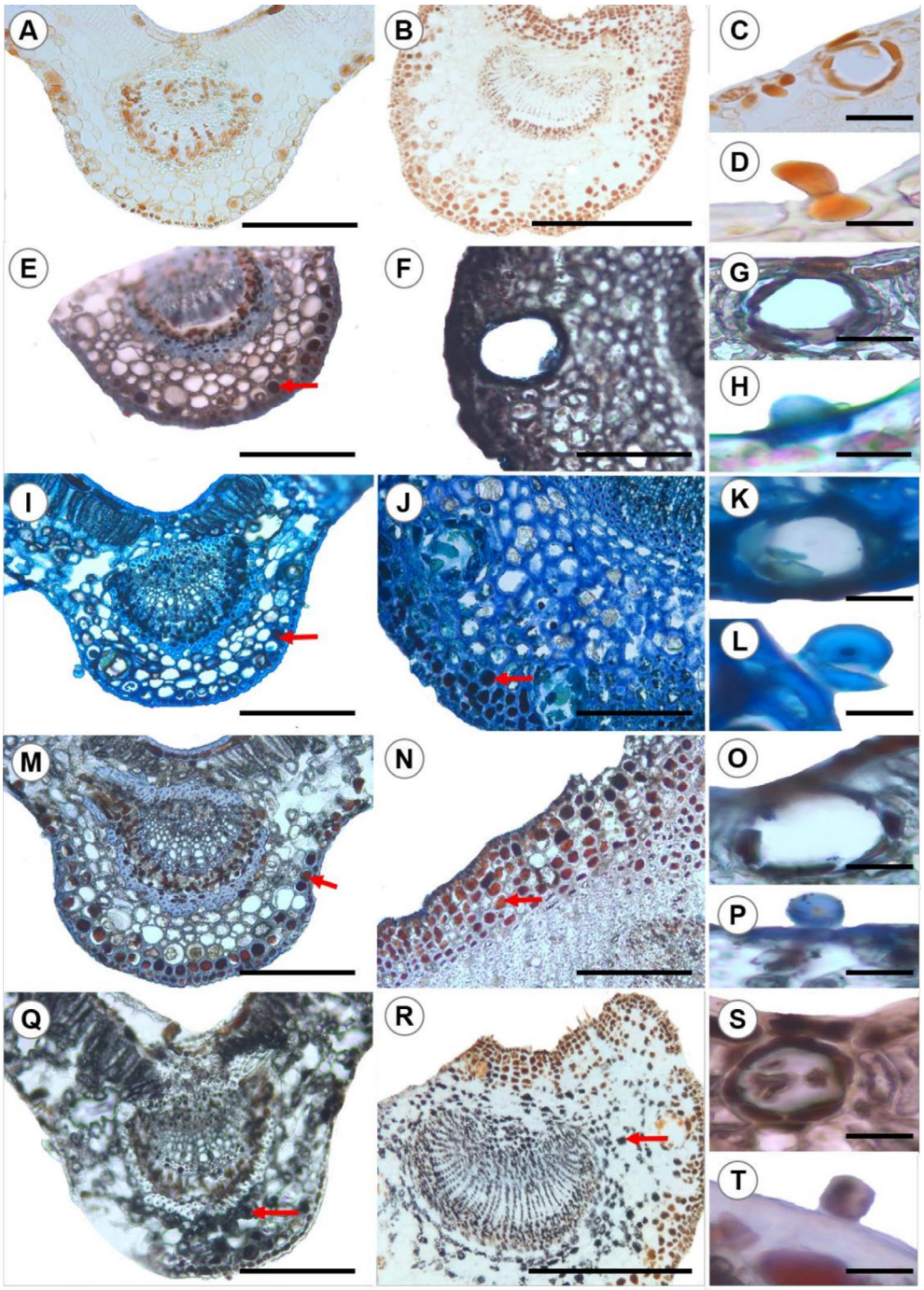


FIGURE 5 | Histochemical tests applied to the leaf of *Myrcia sylvatica* (G. Mey) DC. (A) Blank midrib—secretory epidermis and idioblast. (B) Petiole in white—secretory epidermis and idioblast. (C) Secretory cavity in white. (D) Trichome in white. (E–H) Positive reaction for total lipids. (I–L) Positive reaction for fatty acids. (M, N) Positive reaction for terpenes showing resin oil. (O, P) Positive reaction for terpenes showing essential oil. (Q, R, S, T) Positive reaction for phenolic compounds. Arrow indicating the reaction in secretory idioblasts. Scale bar: 50 μm (C, D, G, H, K, L, O, P, S, T) 100 μm (A, E, I, M, Q) 200 μm (B, F, J, N, R).

oil caused a reduction in the germination rate of *Allium cepa* at concentrations of 187.5, 1500 and 3000 $\mu g\,mL^{-1}$. At the highest concentration tested, there was a 61.6% increase in germination inhibition.

(*E*)-Caryophyllene is a hydrocarbon sesquiterpene. In the steam distillation extraction technique, it had a concentration of 7.22%, and in hydrodistillation its concentration was 4.88%. The difference in concentration suggests that steam distillation favours the retention of this compound, minimising the thermal degradation of volatile compounds [26, 67]. Furthermore, in a previous study, (*E*)-caryophyllene was characterised as the majority compound in the essential oil of *M. sylvatica* leaves [10].

Spathulenol, an oxygenated sesqueterpene, showed significant concentrations in both extraction techniques, with 8.07% in steam distillation and 7.57% in hydrodistillation. The small

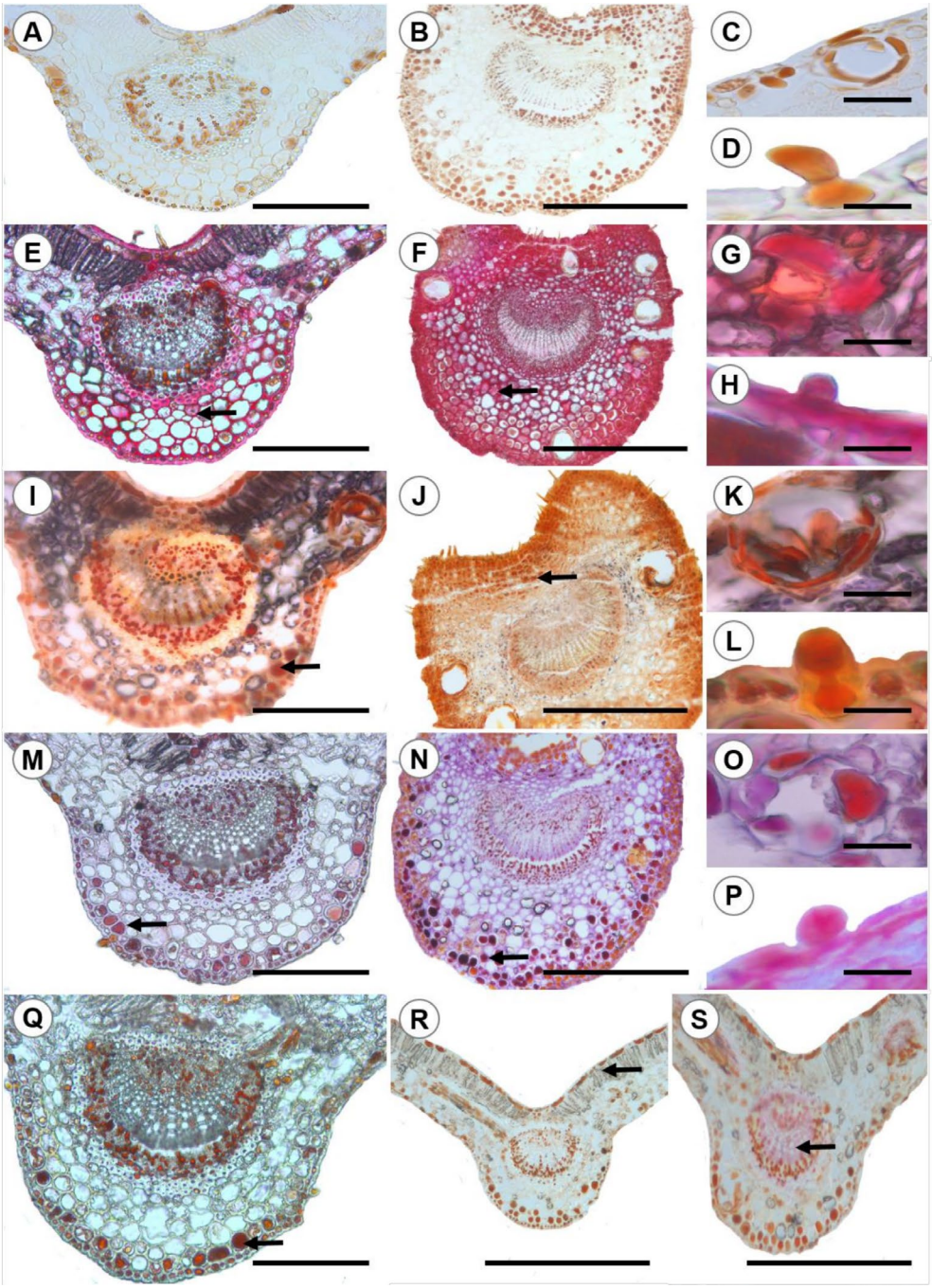


FIGURE 6 | Histochemical tests applied to the leaf of *Myrcia sylvatica* (G. Mey) DC. (A) Central vein in white—secretory epidermis and idioblast. (B) Petiole in white—secretory epidermis and idioblast. (C) Secretory cavity in white, (D) Trichome in white. (E–H) Positive reaction to acid mucilage. (I–L) Positive reaction to alkaloids. (M–P) Positive reaction to total polysaccharides. (Q) Positive reaction to tannin. (R) Positive reaction to starch. (S) Positive reaction to lignin. Arrow indicating reaction in idioblasts. Scale bar: 50 μm (C, D, G, H, K, L, O, P), 100 μm (A, E, I, M, Q), 200 μm (B, R, J, N, R, S).

variation in concentrations suggests that spathulenol maintains its properties and concentrations in a similar way in steam distillation and hydrodistillation [26, 67].

Globulol, an oxygenated sesquiterpene, showed a concentration of 5.74% in hydrodistillation compared to 2.72% in steam distillation. This result shows that the extraction method influences the chemical composition of the essential oil [68], as each extraction technique can favour or reduce the concentration of the constituents depending on their volatility and solubility.

3.3.1 | Statistical Analysis

The correlation matrix reveals highly organised structural patterns of interdependence amongst the analysed chemical compounds, uncovering relationships that go beyond simple linear associations (Figure 8). Two major variable clusters are observed, displaying positive correlations within each group and negative correlations between distinct groups. Compounds such as α-cubenene, δ-bemene, β-bisabolene, α-cadinene, γ-muurolene, and germacrene-D form a tightly intercorrelated set, with correlation

TABLE 2 | Chemical composition of the essential oils of *Myrcia sylvatica* (G. Mey) DC extracted by steam distillation and hydrodistillation.

			Steam distillation	Hydrodistillation
RI_L	RI_C	Extraction method yield chemical compounds	0.24%	0.41%
844[a]	842	Hex-(3*E*)-enol		0.08
853[a]	850	Hex-(3*Z*)-enol		034
864[a]	851	Hex-(2*E*)-enol	1.55	
866[a]	863	Hex-(2*Z*)-enol		0.09
941[a]	944	2-Acetoxyhexane		0.07
988[a]	988	Myrcene		0.03
1187[b]	1183	Hex-(3*Z*)-enyl butyrate		0.01
1195[b]	1193	α-Terpineol		0.02
1335[a]	1331	δ-Elemene	1.71	1.24
1345[a]	1345	α-Cubebene	0.52	0.28
1371[a]	1367	Cyclosativene	0.21	0.19
1374[a]	1373	α-Copaene	0.95	0.55
1378[b]	1378	(3*Z*)-Hexenyl hexenoate	0.11	
1382[a]	1381	β-Bourbonene	0.36	0.33
1389[a]	1388	β-Elemene	2.33	1.95
1405[a]	1401	Sesquithujene		0.02
1406[b]	1404	α-Gurjunene	0.17	0.15
1416[a]	1412	*cis*-α-Bergamotene	0.06	0.06
1424[b]	1420	(*E*)-Caryophyllene	7.24	4.89
1430[b]	1424	γ-Maaliene		0.09
1432[a]	1428	γ-Elemene	2.43	2.66
1432[a]	1431	*trans*-α-Bergamotene	0.7	0.45
1439[a]	1437	Aromadendrene	1.08	0.92
1442[a]	1439	6,9-Guaiadiene	0.72	0.23
1447[a]	1443	Isogermacrene D		0.28
1451[a]	1447	*cis-Muurola-3,5-diene*	0.56	0.5
1454[a]	1450	(*E*)-β-Farnesene	0.55	
1454[b]	1454	α-Humulene	0.87	1.22
1458[a]	1458	*allo*-Aromadendrene	1.4	1.09
1475[a]	1469	γ-Gurjunene	0.86	
1478[b]	1475	γ-Muurolene	1.83	2.34
1480[a]	1481	Germacrene D	10.72	5.52
1483[b]	1484	*trans*-β-Bergamotene		0.21
1492[b]	1490	β-Selinene	3.16	3.92
1496[a]	1492	Viridiflorene	3.04	2.05
1496[b]	1497	α-Zingiberene	14.27	9.14
1500[a]	1498	α-Muurolene	2.66	

(Continues)

TABLE 2 | (Continued)

			Steam distillation	Hydrodistillation
RI_L	RI_C	Extraction method yield chemical compounds	0.24%	0.41%
1506[a]	1503	δ-Amorphene	1.26	0.81
1508[b]	1507	β-Bisabolene	0.78	0.49
1512[a]	1513	γ-Cadinene	1.55	1.25
1518[a]	1519	δ-Cadinene	4.25	3.81
1521[a]	1520	t*rans*-Calamenene	0.57	
1523[a]	1524	β-Sesquiphellandrene	2.7	2.41
1529[a]	1526	(*E*)-γ-Bisabolene	0.57	0.35
1536[b]	1531	*trans*-Cadine-1,4-diene	0.43	0.45
1538[a]	1535	α-Cadinene	0.43	0.43
1544[a]	1540	α-Calacorene	0.56	0.67
1557[b]	1557	Germacrene B	0.92	0.87
1558[a]	1560	*epi*-Longipinanol	0.37	0.56
1561[a]	1563	(*E*)-Nerolidol		0.11
1567[a]	1569	Palustrol	0.7	1.61
1577[a]	1580	Spathulenol	7.56	7.58
1582[a]	1582	Caryophyllene oxide	0.51	0.52
1590[a]	1588	Globulol	2.72	5.74
1594[a]	1596	Viridiflorol	1.34	2.95
1595[a]	1598	Cubeban-11-ol	1.07	1.75
1602[a]	1604	Ledol	0.26	0.66
1609[b]	1607	Rosifoliol	0.84	1.52
1618[a]	1614	1,10-di-*epi*-Cubenol		0.3
1619[b]	1622	Junenol	0.91	1.11
1627[b]	1624	Eremoligenol	0.93	1.48
1627[a]	1627	1-*epi*-Cubenol	1.03	1.77
1632[b]	1633	Muurola-4,10(14)-dien-1-β-ol	0.72	1.3
1639[a]	1637	aromadendrene *allo-epoxide*		0.14
1640[b]	1642	*epi*-α-Cadinol	0.95	1.68
1640[a]	1644	*epi*-α-Muurolol	1	2.4
1644[a]	1648	α-Muurolol	0.64	0.98
1650[b]	1650	Himachalol	0.11	0.31
1652[a]	1659	α-Cadinol	1.83	5.2
1658[a]	1662	Selin-11-en-4-α-ol	1.1	1.28
1658[b]	1666	neo-Intermedeol		0.1
1664[b]	1670	Allohimachalol	0.06	0.86
1671[a]	1677	14-hydroxy-9-*epi*-(*E*)-caryophyllene		0.26
1679[a]	1685	*epi*-α-Bisabolol		0.33

(Continues)

TABLE 2 | (Continued)

RI_L	RI_C	Extraction method yield chemical compounds	Steam distillation 0.24%	Hydrodistillation 0.41%
1685[a]	1686	α-Bisabolol		0.15
1685[b]	1689	Germacra-4(15),5,10(14)-trien-1-α-ol		0.19
1698[a]	1693	(2Z,6Z)-Farnesol		0.27
1700[a]	1697	Eudesm-7(11)-en-4-ol		0.47
1713[a]	1713	(2*E*,6Z)-Farnesal		0.02
1714[a]	1716	Nootkatol		0.13
1730[b]	1722	γ-Costol		0.12
1730[a]	1727	Vetiselinenol		0.05
1733[a]	1729	Isobicyclogermacrenal		0.07
1740[a]	1735	Mint sulphide		0.08
1751[b]	1741	Xanthorrizol		0.1
1752[b]	1754	7,14-Anidro-Amorfo-4,9-dieno		0.12
1767[a]	1762	13-Hydroxyvalencene		0.17
1769[b]	1766	Drimenol		0.22
1779[a]	1770	14-hydroxy-α-muurolene		0.16
1793[a]	1790	(*E*)-Isovalencenol		0.1
		Monoterpene hydrocarbons		0.03
		Oxygenated monoterpenes		0.02
		Sesquiterpene hydrocarbons	72.54	52.16
		Oxygenated sesquiterpenes	24.28	44.12
		Others	1.91	1.05
		Total	98.73	97.38

Note: RIL, retention index of a = Adams library [28]; b = FFNCS library [60]. RIC, retention index calculated from a homologous series of n -alkanes (C8–C40) on a DB5-MS column.

coefficients close to 1 amongst themselves. This systematic co-occurrence suggests that these compounds likely share common biosynthetic pathways or are products of the same enzymatic lineage. The high correlation between α-cubebene and δ-elemene, for instance, may reflect a metabolic origin from a shared precursor, such as farnesyl pyrophosphate (FPP), via the mevalonate pathway, which often yields cyclic sesquiterpenes [69, 70].

On the other hand, compounds like (*E*)-caryophyllene, spathulenol, palustrol, globulol, epi-α-cadinol, selina-6-en-4-ol, and α-muurolol exhibit similarly high positive correlations amongst themselves, forming a distinct, metabolically related group. The simultaneous presence of palustrol and spathulenol, with their strong correlation, suggests either sequential biosynthetic conversion or shared intermediate byproducts in oxidative processes of alcoholic sesquiterpenes. Even more intriguing is the fact that these two major groups are negatively correlated with each other. For example, (*E*)-caryophyllene shows a negative correlation of –1 with α-cubenene and δ-elemene, indicating not only distinct metabolic pathways but also a form of metabolic exclusivity or biochemical antagonism between the biosynthetic routes responsible for their production [71]. This could imply that the production of compounds like (*E*)-caryophyllene occurs at the expense of cubenene biosynthesis, possibly due to direct competition for limiting precursors or opposing regulation of key enzymes [72].

Furthermore, the negative correlation between β-bisabolene and globulol indicates that these compounds are not only formed independently but that the presence of one is systematically associated with the absence of the other. This exclusivity may reflect ecological or adaptive factors, such as chemical specialisations driven by different environmental selective pressures (e.g., defence against herbivores, pollinator attraction, etc.) [73]. Compounds like epi-cubenol and epi-α-muurolol, which are also highly correlated with each other, show marked negative correlations with δ-cadinene and caryophyllene oxide, suggesting that beyond the differentiation between major groups, there are even more specific subdivisions within biosynthetic trajectories.

Overall, the structure of the matrix reveals that the analysed chemical system is highly compartmentalised, with strongly

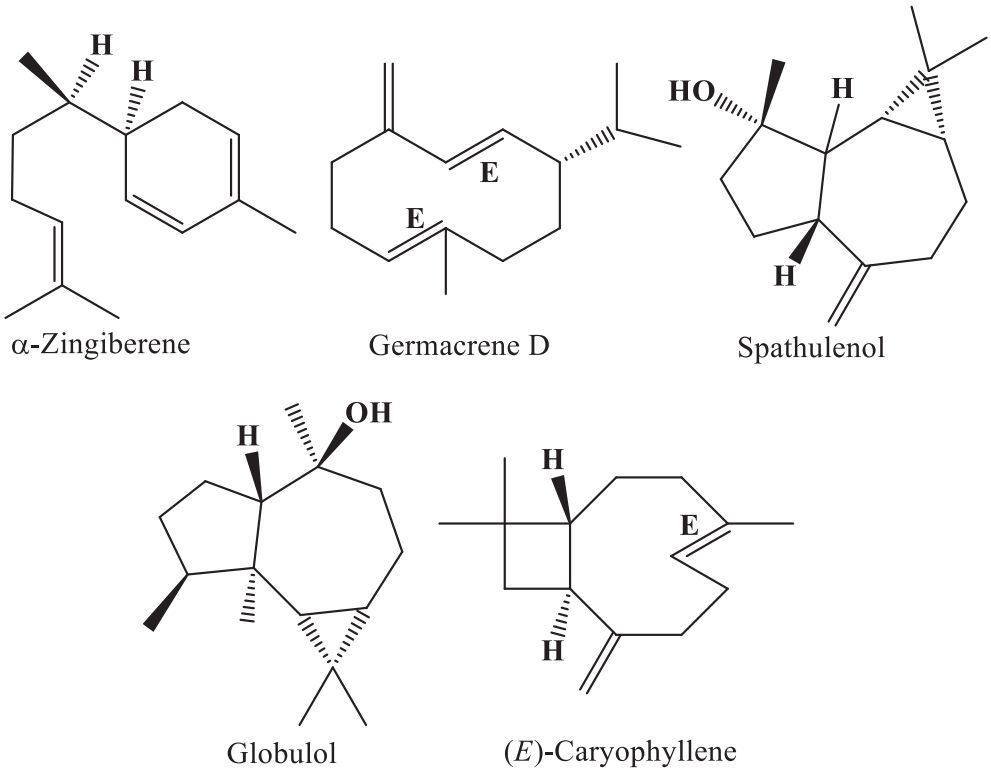


FIGURE 7 | Two-dimensional chemical structure of the main constituents identified in the essential oil of *M. sylvatica*.

structured relationships between compounds. The polarisation in correlations (extreme values with no intermediates) suggests a tightly regulated biochemical system in which groups of compounds are synthesised in a coordinated and mutually exclusive manner. This organisation not only reflects metabolic compartmentalisation but may also indicate functional modularity, with significant implications for chemical ecology, chemotaxonomy (chemotyping), and potential biotechnological applications [73]. Understanding this chemical architecture, based on the observed correlations, provides a solid foundation for future investigations into metabolic regulation, functional diversity, and the biosynthetic origin of the compounds in question.

3.4 | Preliminary Toxicity

In the control test there was no mortality, showing that the use of DMSO is viable as a solvent for the test. The LC_{50} values were obtained by converting the *A. salina* mortality rates into probit units, allowing the regression curve to be drawn as a function of the oil concentrations expressed on a logarithmic scale. Table 3 shows the mortality results and the LC_{50} concentrations.

The essential oils of *M. sylvatica* leaves extracted by hydrodistillation and steam distillation showed LC_{50} of 5.83 and 4.17 $\mu g\,mL^{-1}$, respectively. The oils were toxic to *A. salina*. According to Nguta et al. [74] products that show activity $< 100\,\mu g\,mL^{-1}$have high toxicity compared to products that are $> 1000\,\mu g\,mL^{-1}$ which are considered to have low toxicity.

The toxicity of the essential oils of *M. sylvatica* on *A salina* may be related to the place of collection and, consequently, to the chemical composition of the essential oils, for example, essential oils of *M. sylvatica* collected in the municipality of Bujaru in the state of Pará by Moraes et al. [11] rich in hydrocarbon monoterpenes, and oxygenated monoterpenes showed greater toxicity with an LC_{50} of 2.74 $\mu g\,mL^{-1}$ than the essential oil collected by Rosa et al. [10] in Carolina, Maranhão, in Carolina, Maranhão, which showed a lower toxicity LC_{50} of 79.44 $\mu g\,mL^{-1}$, being an oil rich in (*E*)-caryophyllene (45.88%) and 14-hydroxy-(*Z*)-caryophyllene (10.15%).

This activity may also be related to the presence of the compounds (*E*)-caryophyllene and spathulenol, which show toxic activity in *A. salina* [75]. Germacrene D also shows toxic bioactivity [76]. as well as α-zingiberene, which has the ability to interact with biological systems, causing adverse effects [77, 78]. According to the literature, essential oils rich in sesquiterpenes have toxicological potential in *A. salina* [79, 80].

3.5 | Antioxidant Capacity

Table 4 shows the antioxidant activity of the essential oils. In the $ABTS^{\bullet+}$ radical scavenging test, the essential oil extracted by HD showed an IC_{50} of 8.36 ± 0.50 mg/mL and a Trolox Equivalent Antioxidant Capacity (TEAC) of $834.63 \pm 56.85\,\mu g$ TE/g of essential oil (EO). The essential oil extracted by SD had an IC_{50} of 6.80 ± 0.08 mg/mL and a TEAC of $1026.77 \pm 2.96\,\mu g$ TE/g OE. In the test against $DPPH^{\bullet}$ radicals, the essential oil extracted by HD showed a CI_{50} of 24.62 ± 1.58 mg/mL and the TEAC value was $116.98 \pm 7.47\,\mu g$ TE/g OE, while the essential oil extracted by SD showed a CI_{50} of 12.80 ± 0.19 mg/mL and TEAC $225.00 \pm 3.25\,\mu g$ TE/g OE. These results are illustrated in Figures 9 and 10, which show the percentage of radical

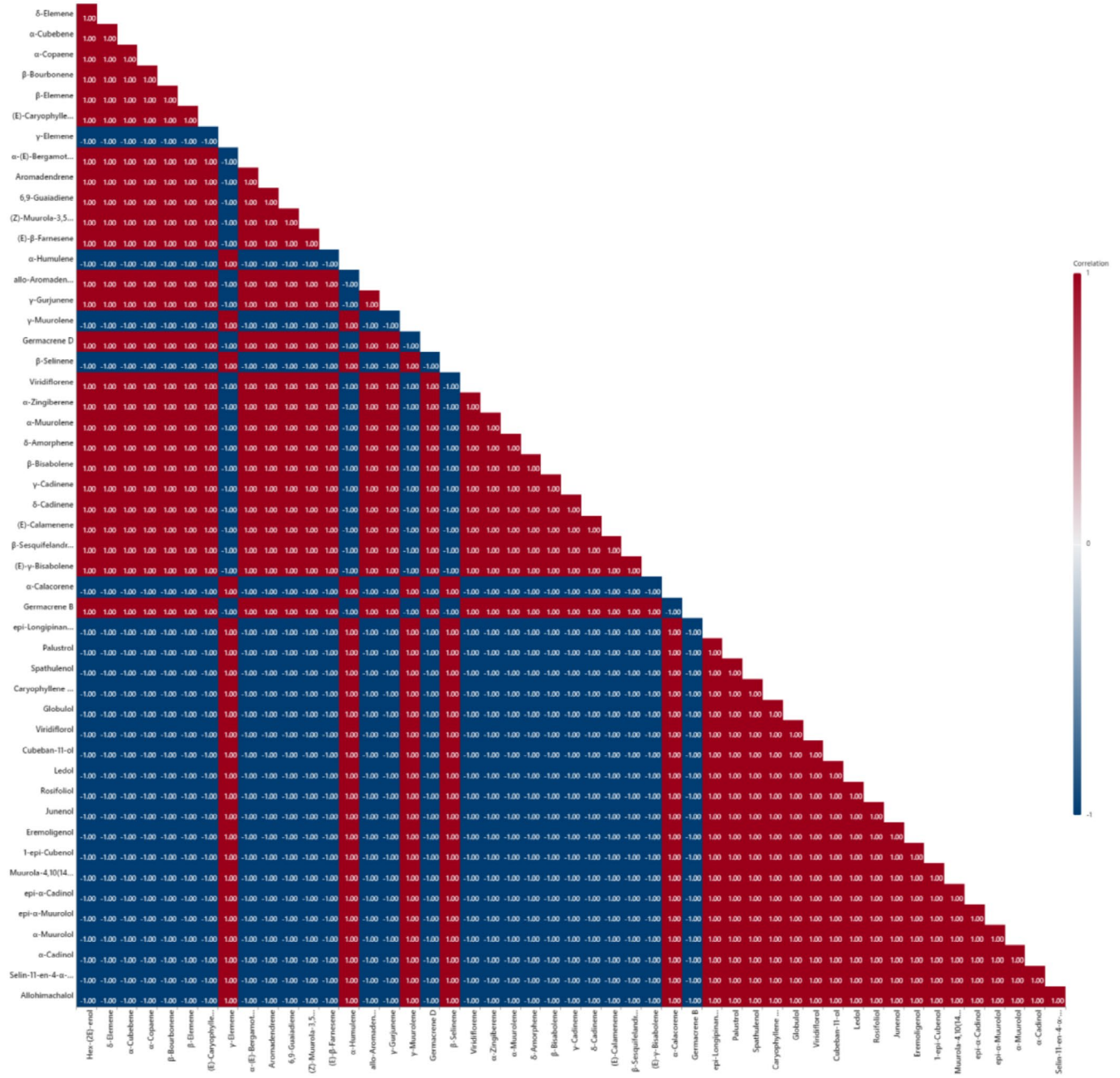


FIGURE 8 | Correlogram of the correlation matrix between the identified chemical compounds. The colour represents the strength and direction of the Pearson correlation between pairs of compounds, with shades of red indicating positive correlations and shades of blue indicating negative correlations. Values equal to 1 indicate maximum positive correlation, while values equal to −1 indicate maximum negative correlation. The formation of distinct blocks of compounds with high correlation within the groups and negative correlation between different groups is observed, indicating possible coordinated biosynthetic relationships and metabolic exclusivity between chemical sets.

inhibition as a function of the essential oil concentrations. There was no significant difference in the percentage of free radical inhibition by the essential oils obtained from HD and SD at the concentrations tested.

The antioxidant activity displayed by the essential oils can be attributed to their constituents. In particular, the oil obtained by SD, characterised by a high percentage of sesquiterpene hydrocarbons (72.42%) and oxygenated sesquiterpenes (25.65%), was more efficient in inhibiting both types of radicals. These results can be attributed mainly to the oxygenated compounds present in the oil, which generally have greater antioxidant activity than hydrocarbons of the same class [81]. Although isolated sesquiterpene hydrocarbons such as Germacrene D and (*E*)-caryophyllene do not show considerable antioxidant activity, essential oils rich in sesquiterpenes have shown considerable antioxidant activity against $ABTS^{\bullet+}$ and $DPPH^{\bullet}$ radicals [82–84].

The germacrene D, a sesquiterpene hydrocarbon, is one of the main constituents of *M. sylvatica* essential oil, with a concentration of 10.72% in steam distillation and 5.51% in hydrodistillation. In a study carried out with *Eugenia patrissi*, the essential oil showed germacrene D (20.03%) as the majority compound;

TABLE 3 | Preliminary toxicity of *Myrcia sylvatica* (G. Mey) DC, essential oil to *Artemia salina*.

Essential Oil	Concentration ($\mu g\,mL^{-1}$)	Mortality (%)	$LC_{(50)}$ ($\mu g\,mL^{-1}$)
HD	100	100	5.83 ± 0.31
	50	100	
	25	90	
	10	46.67	
	5	33.33	
	1	13.33	
SD	100	100	4.17 ± 1.16
	50	100	
	25	96,67	
	10	70	
	5	43.33	
	1	10	

Note: Values are expressed as mean and standard deviation ($n = 3$) of preliminary toxicity.

TABLE 4 | Antioxidant activity of *Myrcia sylvatica* (G. Mey) DC. essential oil.

	IC_{50} (mg/mL)		TEAC (μg TE/g OE)	
Essential oil	**ABTS**	**DPPH**	**ABTS**	**DPPH**
HD	8.36 ± 0.50	24.62 ± 1.58	834.63 ± 56.85	116.98 ± 7.47
SD	6.80 ± 0.08	12.80 ± 0.19	1026.77 ± 2.96	225.00 ± 3.25

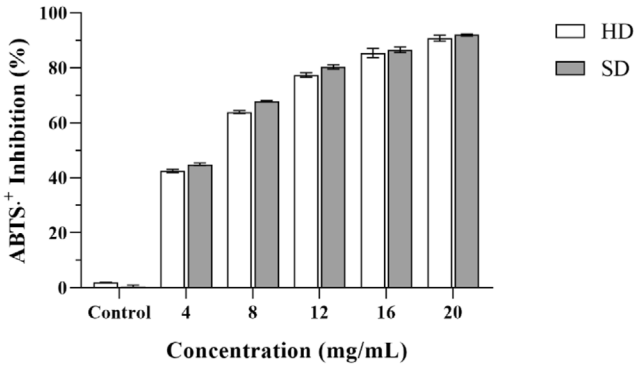


FIGURE 9 | Antioxidant activity of the essential oil of *Myrcia sylvatica* (G. Mey) DC, obtained by hydrodistillation (HD), assessed by the $ABTS^{\bullet+}$ assay, expressed as mean and standard deviation ($n = 2$).

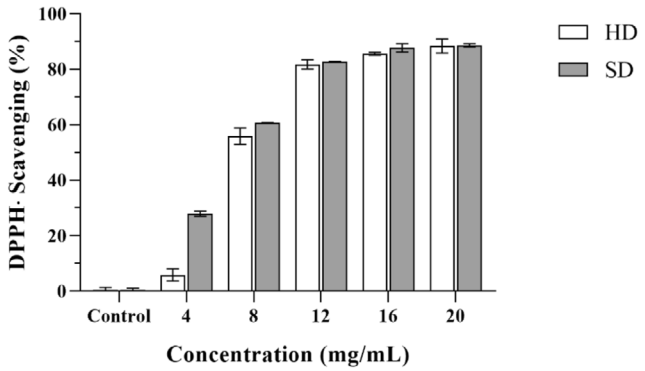


FIGURE 10 | Antioxidant activity of *Myrcia sylvatica* (G. Mey) DC, essential oil, obtained by steam distillation (SD), assessed by the $DPPH^{\bullet}$ assay, expressed as mean and standard deviation ($n = 2$).

the essential oil of the species obtained significant antioxidant activity, with inhibition of 31.4 ± 0.1 $ABTS^{\bullet+}$ and 99.0 ± 0.099 ($DPPH^{-}$), antioxidant capacity equivalent to the trolox standard in the $DPPH^{\bullet}$ assay [85].

On the other hand, even with a higher percentage of oxygenated sesquiterpenes (45.02%), the essential oil obtained by HD showed lower antioxidant activity in the two methods analysed, indicating the antagonistic and/or synergistic influences that each antioxidant compound present in the mixture can exert on the others and, consequently, on the overall effect of the interaction with the free radical [86, 87]. Previous studies also report that *M. sylvatica* has antioxidant activity, mainly associated with the high concentration of hydrocarbon and oxygenated sesquiterpenes in its composition [11].

The oils obtained by the two extraction techniques were more effective in the $ABTS^{\bullet+}$ radical scavenging tests than in the $DPPH^{\bullet}$ radical scavenging tests. The difference in results can be attributed to the nature of the reaction mechanism for eliminating each of the radicals, considering that, although both tests involve the transfer of a single electron (SET) and the transfer of a hydrogen atom (HAT) from the antioxidant substances, both types of mechanisms can occur simultaneously at different rates during

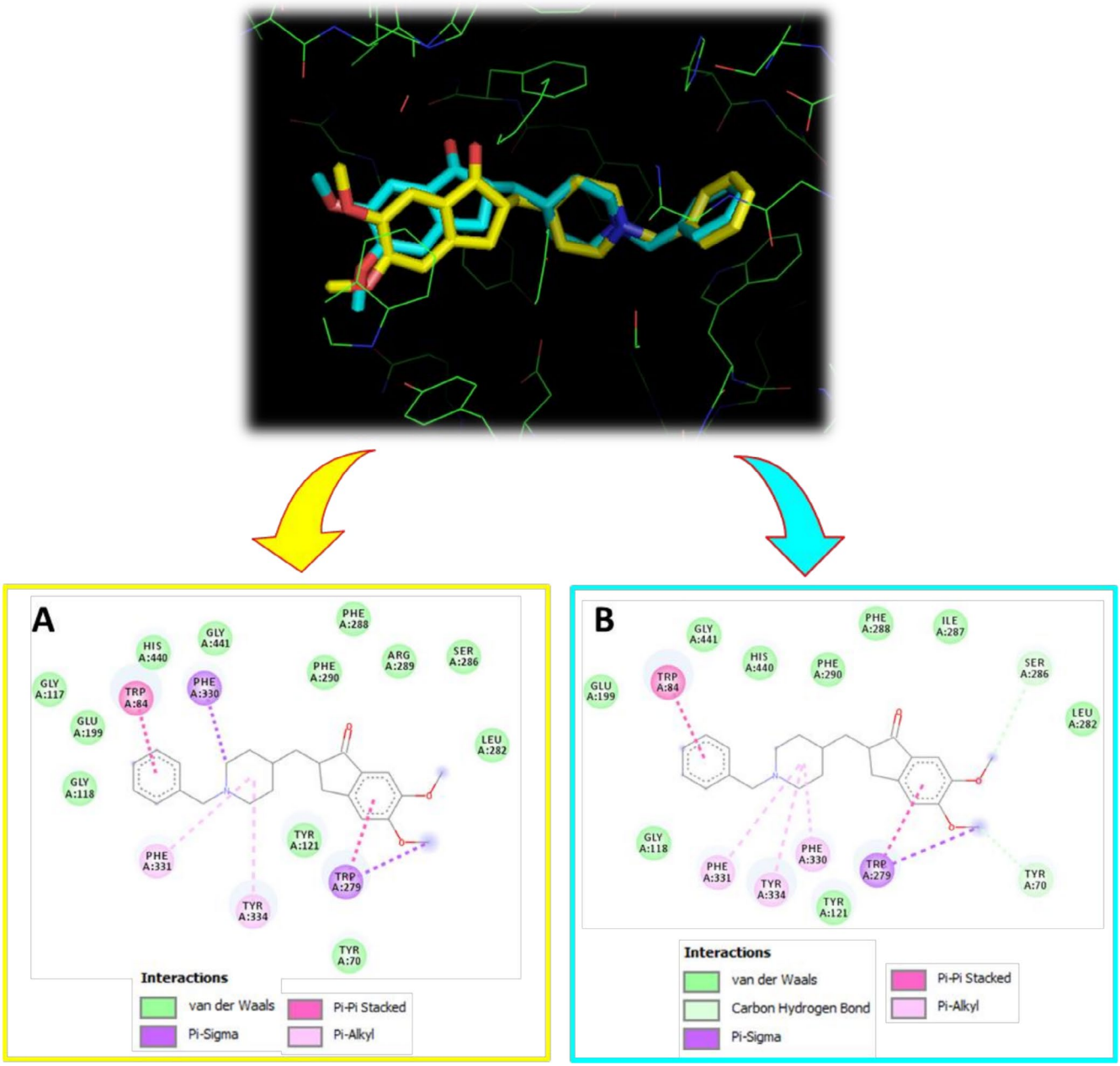


FIGURE 11 | 2D model of different interactions formed by the co-crystallised 'donepezil' (yellow colour) (A) and the re-docked 'donepezil' (cyan colour) (B) within the active site of AChE (pdb: 1EVE).

the reaction, depending on the nature of the radical and the antioxidant, and the conditions of the reaction medium [88–91].

3.6 | Computational Approach

3.6.1 | Docking Validation

To enhance our understanding of the intricate ligand-protein binding interactions, the *in silico* docking simulations were performed. To validate the procedure of this technique, the docked 'donepezil' (Figure 11B) structure was overlayed with 'donepezil' obtained from the crystal structure of the AChE (Figure 11A). We displayed the interactions formed originally between the

TABLE 5 | Docking results of the docked ligands with their binding energy scores.

Docked ligan	binding energies (kcal mol^{-1})
α-Zingiberene	−8.1
Germacrene D	−8.0
Spathulenol	−8.9
Globulol	−8.3
(*E*)-Caryophyllene	−8.1
Co-crystallised ligand «Donepezil»	−9.6

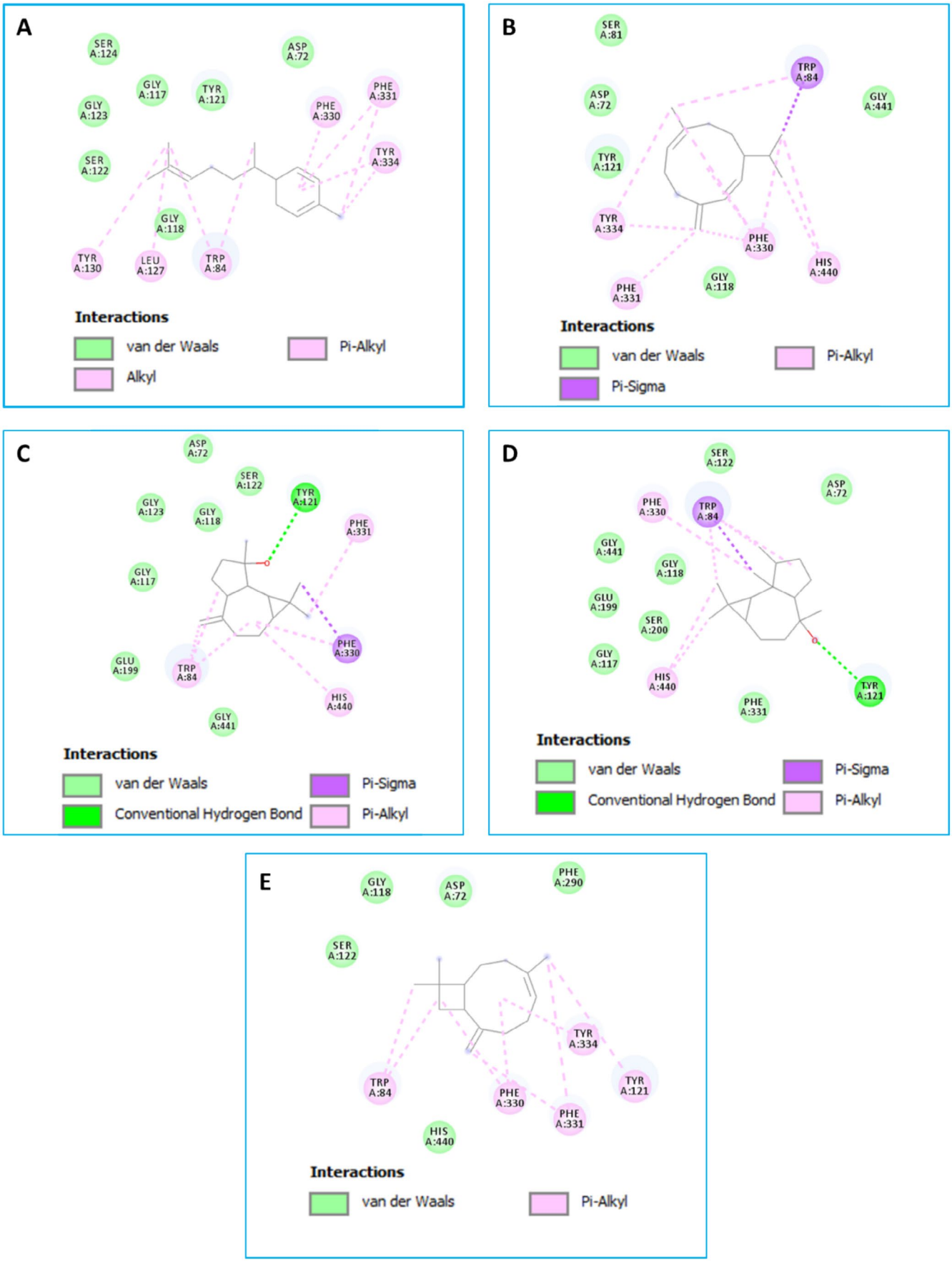


FIGURE 12 | 2D binding modes of the most bioactive compounds: A: α-zingiberene, B: Germacrene D, C: Spathulenol, D: Globulol and E: (*E*)-caryophyllene.

TABLE 6 | In silico ADME analysis of the main phytoligands.

Entry	A	B	C	D	E
GI absorption*	Low	Low	High	High	Low
P–gp substrate*	No	No	No	No	No
BBB permeant*	No	No	Yes	Yes	No
CYP1A2 inhibitor*	No	No	No	No	No
CYP2C19 inhibitor*	Yes	No	Yes	Yes	Yes
CYP2C9 inhibitor*	Yes	Yes	No	Yes	Yes
CYP2D6 inhibitor*	No	No	No	No	No
CYP3A4 inhibitor*	No	No	No	No	No
Log Kp (cm/s)[a]*	−3.88	−4.18	−5.44	−4.81	−4.44
Lipinski**	Yes	Yes	Yes	Yes	Yes
Veber**	Yes	Yes	Yes	Yes	Yes
Egan**	Yes	Yes	Yes	Yes	Yes
Bioavailability Score**	0.55	0.55	0.55	0.55	0.55
TPSA (Å^2)***	00.00	00.00	20.23	20.23	00.00
Consensus Log *Po*/w****	4.44	4.30	3.29	3.73	4.24

Note: a: skin permeability, A: α-zingiberene, B: germacrene D, C: spathulenol, D: globulol and E: (*E*)-caryophyllene, Pharmacokinetics*, Druglikeness**, Physicochemical Properties*** and Lipophilicity****.

co-crystallised molecule and the targeted enzyme in order to show the similarity through the positioning and the residues involved in the interactions. From the molecular docking outcomes, it should be noted that the redocked 'donepezil' interacts favourably with the receptor; this ligand exhibited similar interactions to those found originally in the crystal structure. Furthermore, the result of the superposition figure displays that the root mean square deviation 'RMSD' between the two ligands (cyan: re-docked and yellow: co-crystallised) is minimal.

3.6.2 | Docking Results Analysis

Based on the free-binding energy values, the obtained outcomes indicate that the ligands spathulenol (−8.9 kcal mol^{-1}) were found to be the most bioactive compound as Table 5 shows. This docked molecule is involved in a conventional hydrogen bond with Tyr121. The interesting potential of spathulenol is also explained by the formation of some other contacts, such as Pi-Sigma with Phe330 and Pi-Alkyls with Trp84, Phe330, Phe331 and His440 (Figure 12C). By showing almost the same interactions, as Figure 12D exhibits, globulol was considered the second effective ligand while the two phytocompounds α-zingiberene and (*E*)-caryophyllene displayed the third best anti-AChE potentials by the formation of some hydrophobic contacts: Alkyl and Pi-Alkyl as detailed in Figure 12A,E. On the other hand, Germacrene D was found to be the least active compound by showing a Pi-Sigma interaction with Trp84 in addition to Pi-Alkyl contacts with Phe330, Phe331, Tyr334 and His440 respectively.

Although all docked phytoligands cannot show scores comparable to the reference (co-crystallised ligand), they were able to form very interesting interactions in comparison with the interactions formed by Donepezil, in particular with the two alcohols: spathulenol and globulol which formed H-bonds. All these outputs and findings display the importance of the tested phytocompounds in the inhibition of AChE.

3.6.3 | Predictive ADME Analysis

The forecasting of ADME (absorption, distribution, metabolism and excretion) data of the major phytocompounds has been estimated. The predicted descriptors including their pharmacokinetic and druglikeness properties are shown in Table 6. All tested ligands were found to correctly meet Lipinski's rule, and so share 'topological polar surface area' (TPSA) values of 00.00 to 20.23Å^2, supporting the probability of having predicted high passive oral absorption, which is expressed by the consensus Log Po/w in the range 3.29 to 4.44. Furthermore, the bioavailability score of 0.55 indicates higher bioactivity of the molecule. As noted in Table 6, there is no P-glycoprotein (P–gp) substrate; this finding suggests good intestinal absorption of compounds and bioavailability. Additionally, all tested ligands displayed low gastrointestinal absorption (GI) except for globulol. This compound in addition to spathulenol was predicted to cross the blood–brain barrier (BBB). Further, almost all tested compounds were found to not inhibit the main cytochrome (CYP 450) enzymes: CYP1A2, CYP2C19, CYP2C9, CYP2D6 and CYP3A4. The radar plot (Figure 13), shows that all tested molecules are in the pink zone, confirming their better drug-likeness with a good bioavailability profile. On the other hand, Figure 14 exhibits the BOILED-EGG curve and the BBB penetration, GI absorption (HIA) of the substances may be predicted by this method. Indeed, there are two areas: one for the GI absorption zone (HIA) and the other for BBB penetration (yolk). Neither 'GI absorption' nor 'BBB penetration' is indicated if any component is found in the grey zone. According to the results obtained, two out of five phytoligands: the two alcohols, 'spathulenol' and 'globulol,' appeared in the yellow region (yolk) with a red point that indicated their high probability of brain penetration (BB) acting as a non-substrate of P–gp.

4 | Conclusion

This study offers a pioneering and integrative characterisation of *Myrcia sylvatica*, demonstrating its taxonomically relevant anatomical features and revealing secretory structures associated with a diversity of bioactive metabolites. The essential oils showed chemical variability depending on the extraction method, with a predominance of sesquiterpenes that strongly influenced both antioxidant and toxicological profiles. The steam-distilled oil exhibited superior biological activity, particularly

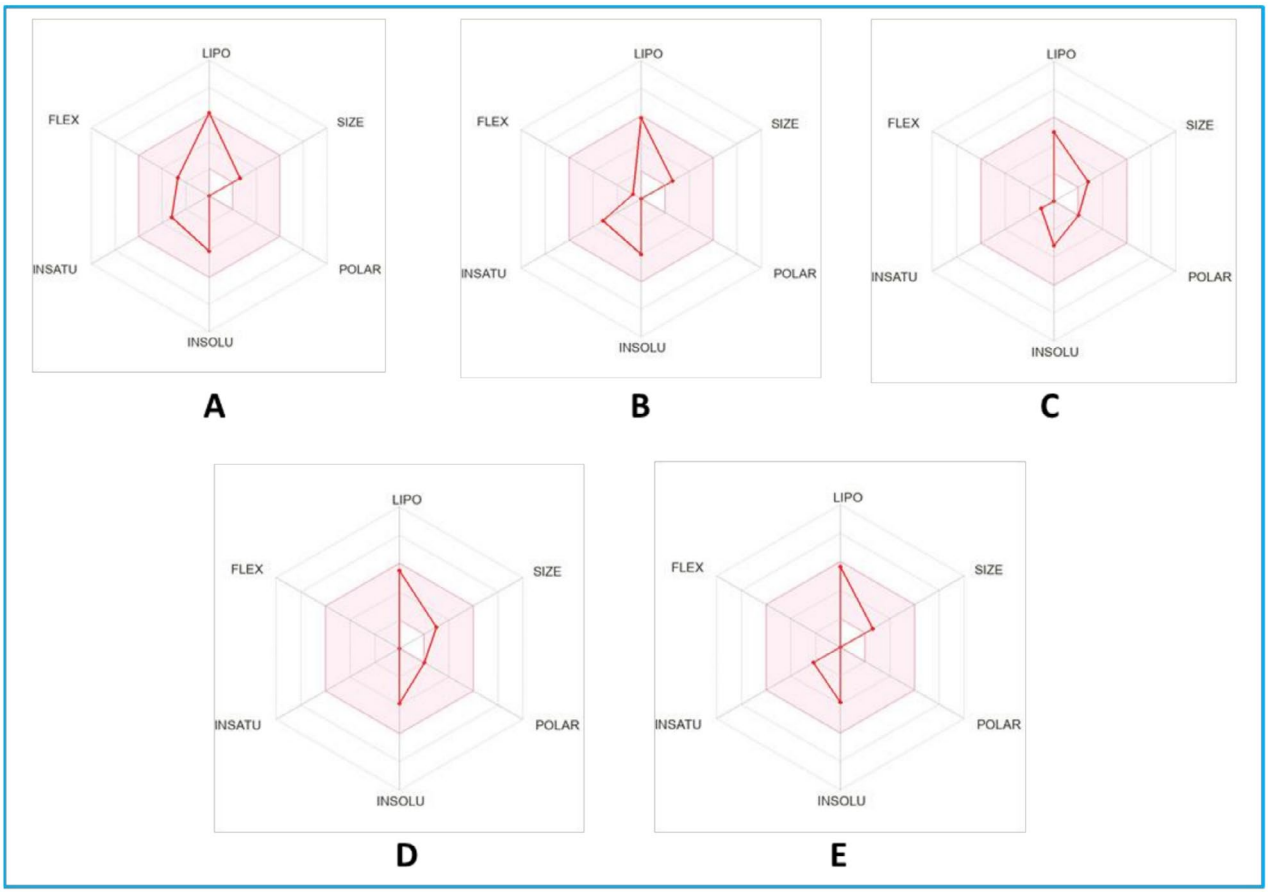


FIGURE 13 | Bioavailability radar of the main phytoconstituants: (A) α-zingiberene, (B) germacrene D, (C) spathulenol, (D) globulol and (E) (*E*)-caryophyllene.

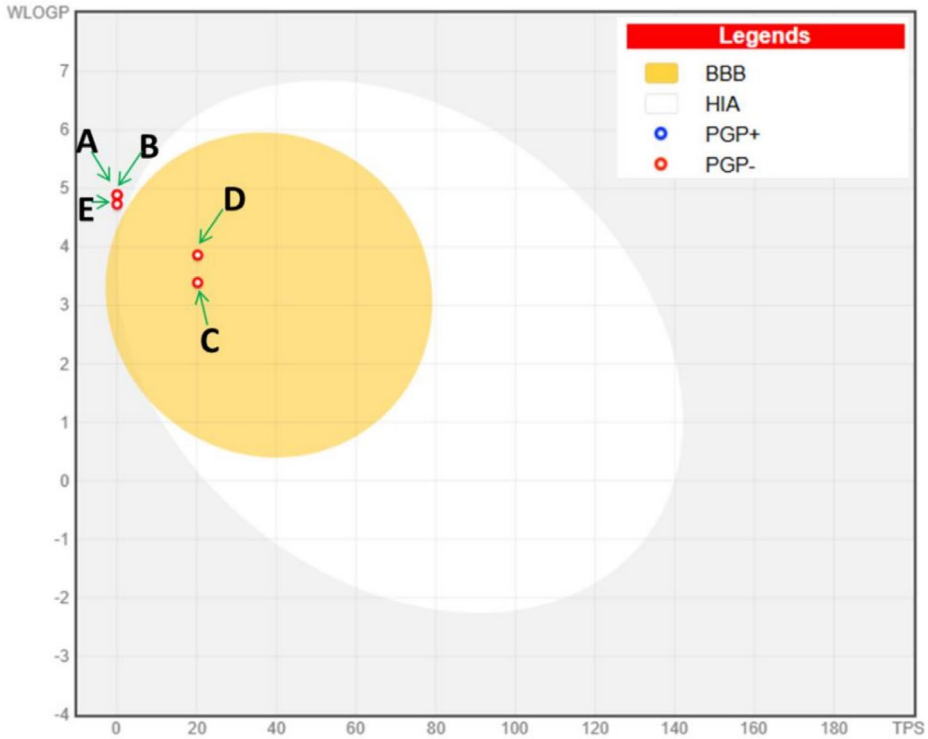


FIGURE 14 | Boiled-egg graph of the main phytoconstituents: (A) α-zingiberene, (B) germacrene D, (C) spathulenol, D: globulol and E: (*E*)-caryophyllene.

in radical scavenging and toxicity assays. Furthermore, molecular docking simulations and ADME predictions revealed that compounds such as spathulenol and globulol possess strong potential as acetylcholinesterase inhibitors, with desirable pharmacokinetic properties. These novel findings not only deepen our understanding of the chemical ecology of *M. sylvatica* but also highlight its potential for pharmaceutical and biotechnological applications. This work expands the scientific basis for the valorisation and sustainable use of Amazonian biodiversity. However, it is important to recognise that acetylcholinesterase represents only one of several toxicologically relevant molecular targets. The present study did not explore other possible biochemical pathways involved in the observed biological effects. Future research should therefore investigate additional molecular targets and mechanistic interactions to more fully elucidate the therapeutic potential and safety profile of *M. sylvatica* and its bioactive constituents.

Author Contributions

E.J.B.S., Z.A.C., E.S.C.G., L.S.C., M.H., H.E., R.K., A.S.B., K.S.S.V., E.H.A.A. and M.S.O. contributed to conceptualisation, investigation, methodology, and writing of the original draft, as well as reviewing and editing the manuscript. M.H. and H.E. also contributed to computational analyses and in silico validation. R.K. additionally contributed to obtaining resources. E.H.A.A. and M.S.O. also contributed to project supervision and administration.

Acknowledgements

The author, Mozaniel Santana de Oliveira thanks PDPG-POSDOC—Programa de Desenvolvimento da Pós-Graduação (PDPG) Pós-Doutorado Estratégico, as well as CAPES for the scholarship (process number: 88887.852405/2023-00). The authors thank CAPES process number 001. Coordenação de Aperfeiçoamento de Pessoal de Nível Superior (CAPES), no âmbito do Programa de Desenvolvimento da Pós-Graduação da Amazônia Legal (PDPG-AL), Plano de Desenvolvimento da Pós-Graduação do Museu Paraense Emílio Goeldi, proposta Estudos integrados da biodiversidade vegetal para conservação e manejo da Amazônia (88887.510208/2020-00). The Article Processing Charge for the publication of this research was funded by the Coordenação de Aperfeiçoamento de Pessoal de Nível Superior - Brasil (CAPES) (ROR identifier: 00x0ma614).

Funding

This work was supported by Coordenação de Aperfeiçoamento de Pessoal de Nível Superior, 88887.852405/2023-00.

Ethics Statement

The authors have nothing to report.

Conflicts of Interest

The authors declare no conflicts of interest.

Data Availability Statement

The data that support the findings of this study are available from the corresponding author upon reasonable request.

References

1. J. Bao, B. O'Donohue, K. D. Sommerville, N. Mitter, C. O'Brien, and A. Hayward, "Tissue Culture Innovations for Propagation and Conservation of Myrteae—A Globally Important Myrtaceae Tribe," *Plants* 13 (2024): 2244, https://doi.org/10.3390/plants13162244.

2. J. D. d. O. Melo, A. M. S. Stadnik, and N. Roque, "Myrtaceae Juss. In Restinga of Bahia: Diversity, Taxonomy, and Distribution," *Acta Botânica Brasílica* 37 (2023): e20220194, https://doi.org/10.1590/1677-941x-abb-2022-0194.

3. L. Anjos da Silva, R. Santos da Silva, M. Rodrigues de Oliveira, A. C. Guimarães, and R. Takeara, "Chemical Composition and Biological Activities of Essential Oils From Myrtaceae Species Growing in Amazon: An Updated Review," *Journal of Essential Oil Research* 35 (2023): 103–116, https://doi.org/10.1080/10412905.2023.2167880.

4. A. Ghani, M. J. Saharkhiz, M. Hassanzadeh, and K. Msaada, "Changes in the Essential Oil Content and Chemical Compositions of *Echinophora platyloba* DC. During Three Different Growth and Developmental Stages," *Journal of Essential Oil Bearing Plants* 12 (2009): 162–171, https://doi.org/10.1080/0972060X.2009.10643706.

5. E. d. J. B. dos Santos, F. W. F. Bezerra, L. R. R. da Silva, et al., "Exploring the Potential of *Myrcia* Genus Essential Oils: A Review of Biological Activities and Recent Advances," *Molecules* 29 (2024): 2720, https://doi.org/10.3390/molecules29122720.

6. J. S. da Costa, J. J. da S. Freitas, W. N. Setzer, J. K. R. da Silva, J. G. S. Maia, and P. L. B. Figueiredo, "Variability in the Chemical Composition of *Myrcia sylvatica* (G. Mey) DC. Essential Oils Growing in the Brazilian Amazon," *Molecules* 27 (2022): 8975, https://doi.org/10.3390/molecules27248975.

7. L. A. da Silva, J. D. A. Raposo, L. P. G. Campos, E. C. da Conceição, R. B. de Oliveira, and R. H. V. Mourão, "Atividade Antioxidante do Óleo Essencial de *Myrcia sylvatica* (G. Mey.) DC. por Diferentes Métodos de Análises Antioxidantes (ABTS, DPPH, FRAP, β-Caroteno/Ácido Linoleico)," *Revista Fitos* 12 (2018): 117–126, https://doi.org/10.5935/2446-4775.20180011.

8. L. B. Jerônimo, J. S. da Costa, L. C. Pinto, et al., "Antioxidant and Cytotoxic Activities of Myrtaceae Essential Oils Rich in Terpenoids From Brazil," *Natural Product Communications* 16 (2021): 1934578X21996156, https://doi.org/10.1177/1934578X21996156.

9. E. M. H. Saccol, C. Toni, T. S. Pês, et al., "Anaesthetic and Antioxidant Effects of *Myrcia sylvatica* (G. Mey.) DC. And *Curcuma longa* L. Essential Oils on Tambaqui (*Colossoma macropomum*)," *Aquaculture Research* 48 (2017): 2012–2031, https://doi.org/10.1111/are.13034.

10. C. S. Rosa, K. S. Veras, P. R. Silva, et al., "Composição Química e Toxicidade Frente *Aedes aegypti* L. e *Artemia salina* Leach do óleo Essencial das Folhas de *Myrcia sylvatica* (G. Mey.) DC," *Revista Brasileira de Plantas Medicinais* 18 (2016): 19–26, https://doi.org/10.1590/1983-084X/15_006.

11. Â. A. B. de Moraes, O. O. Ferreira, L. S. da Costa, et al., "Phytochemical Profile, Preliminary Toxicity, and Antioxidant Capacity of the Essential Oils of *Myrciaria floribunda* (H. West ex Willd.) O. Berg. and *Myrcia sylvatica* (G. Mey) DC, (Myrtaceae)," *Antioxidants* 11 (2022): 2076, https://doi.org/10.3390/antiox11102076.

12. D. Johansen, *Plant Microtechnique* (Mc-Graw-Hillbook Company, 1940).

13. R. D. Lillie, *Histopathologic Technic and Practical Histochemistry*, 3rd ed. (Blakiston Division, McGraw-Hill, 1965).

14. G. Spicher and D. Gerlach, "Botanische Mikrotechnik – Eine Einführung. 3., Unveränderte Auflage. Georg Thieme Verlag, Stuttgart 1984. 311 Seiten, mit 45 Abb., Flexibles Taschenbuch DM 26,80," *Starch – Stärke* 37 (1985): 34, https://doi.org/10.1002/star.19850370120.

15. J. E. Kraus and M. P. P.-S. Arduin, *Basic Manual of Methods in Plant Morphology*, 1st ed. (EDUR, 1997).

16. G. L. Franklin, "Preparation of Thin Sections of Synthetic Resins and Wood-Resin Composites, and a New Macerating Method for Wood," *Nature* 155 (1945): 51.

17. M. J. Purvis, D. C. Collier, and D. Walls, *Laboratory Techniques in Botany*, 1st ed. (Butterworths, Lodon, 1964).

18. A. G. E. Pearse, *Histochemistry, Theoretical and Applied: Preparative and Optical Technology*, 1st ed. (Churchill Livingstone, 1968).

19. A. J. Cain, "The Use of Nile Blue in the Examination of Lipids," *Quarterly Journal of Microscopical Science* 3 (1947): 383–392, https://doi.org/10.1242/jcs.s3-88.3.383.

20. R. David and J. P. Carde, "Histochimie-coloration differentielle des inclusions lipidiques et terpeniques des pseudophylles du pin maritime au moyen du reactif NADI," *Comptes Rendus Hebdomadaires Des Seances De L Academie Des Sciences* 258, no. 4 (1964): 1338.

21. M. E. Mace and C. R. Howell, "Histochemistry and Identification of Condensed Tannin Precursors in Roots of Cotton Seedlings," *Canadian Journal of Botany* 52 (1974): 2423–2426, https://doi.org/10.1139/b74-314.

22. M. Gregory and P. Baas, "A Survey of Mucilage Cells in Vegetative Organs of the Dicotyledons," *Israel Journal of Botany* 38 (1989): 125–174, https://doi.org/10.1080/0021213X.1989.10677119.

23. J. F. A. McManus, "Histological and Histochemical Uses of Periodic Acid," *Stain Technology* 23 (1948): 99–108, https://doi.org/10.3109/10520294809106232.

24. M. Furr and P. G. Mahlberg, "Histochemical Analyses of Laticifers and Glandular Trichomes in *Cannabis sativa*," *Journal of Natural Products* 44 (1981): 153–159, https://doi.org/10.1021/np50014a002.

25. C. J. Chamberlain, *Gymnosperms: Gymnosperms, Structure and Evolution*, 1st ed. (University of Chicago Press, 1935), https://doi.org/10.1126/science.82.2123.225.

26. M. Santana de Oliveira, V. M. Pereira da Silva, L. Cantão Freitas, S. Gomes Silva, J. Nevez Cruz, and E. H. de Aguiar Andrade, "Extraction Yield, Chemical Composition, Preliminary Toxicity of *Bignonia nocturna* (Bignoniaceae) Essential Oil and In Silico Evaluation of the Interaction," *Chemistry & Biodiversity* 18 (2021): e2000982, https://doi.org/10.1002/cbdv.202000982.

27. J. N. Cruz, M. S. de Oliveira, S. F. M. Pereira, O. O. Ferreira, R. R. Lima, and E. H. A. de Andade, "Evaluation of Yield, Chemical Composition and Antioxidant Capacity of the Essential Oil From Leaves and Fruits (Seed and Bark) of *Virola sebifera* Aubl. (Myristicaceae), flavour," *Fragrance Journal* 40 (2025): 892–904, https://doi.org/10.1002/ffj.3871.

28. R. P. Adams, *Identification of Essential Oil Components by Gas Chromatography/Mass Spectorscopy*, 4th ed. (Allured Publishing Corporation, 2007), https://books.google.com.br/books?id=9ut3PQAACAAJ.

29. K. Mesquita, B. Feitosa, J. Cruz, et al., "Chemical Composition and Preliminary Toxicity Evaluation of the Essential Oil From Peperomia Circinnata Link var. Circinnata. (Piperaceae) in *Artemia salina* Leach," *Molecules* 26 (2021): 7359, https://doi.org/10.3390/molecules26237359.

30. E. M. Kuskoski, A. G. Asuero, A. M. Troncoso, J. Mancini-Filho, and R. Fett, "Aplicación de diversos métodos químicos para determinar actividad antioxidante en pulpa de frutos," *Ciência e Tecnologia de Alimentos* 25 (2005): 726–732, https://doi.org/10.1590/S0101-20612005000400016.

31. W. Brand-Williams, M. E. Cuvelier, and C. Berset, "Use of a Free Radical Method to Evaluate Antioxidant Activity," *LWT – Food Science and Technology* 28 (1995): 25–30, https://doi.org/10.1016/S0023-6438(95)80008-5.

32. O. Trott and A. J. Olson, "AutoDock Vina: Improving the Speed and Accuracy of Docking With a New Scoring Function, Efficient Optimization, and Multithreading," *Journal of Computational Chemistry* 31 (2010): 455–461, https://doi.org/10.1002/jcc.21334.

33. G. Kryger, I. Silman, and J. L. Sussman, "Structure of Acetylcholinesterase Complexed With E2020 (Aricept): Implications for the Design of New Anti-Alzheimer Drugs," *Structure* 7 (1999): 297–307, https://doi.org/10.1016/S0969-2126(99)80040-9.

34. L. J. Gatto, V. B. Bobek, J. M. Budel, et al., "Contribution to the Identification of the Species *Myrcia hatschbachii* D. Legrand (Myrtaceae): Anatomical and Histochemical Analyses," *Ciência e Natura* 43 (2021): e75, https://doi.org/10.5902/2179460X43417.

35. V. D. O. T. Lemos, d. E. M. P. Lucena, O. H. Bonilla, B. Edson-Chaves, and M. A. Freitas, "Anatomia ecológica foliar de *Myrcia guianensis* (Aubl.) DC. na Restinga Cearense," *Ciência Florestal* 30 (2020): 307, https://doi.org/10.5902/1980509830997.

36. N. P. Esposito-Polesi, R. R. Rodrigues, and M. de Almeida, "Anatomia ecológica da folha de *Eugenia glazioviana* Kiaersk (Myrtaceae)," *Revista Árvore* 35 (2011): 255–263, https://doi.org/10.1590/S0100-67622011000200010.

37. P. F. Simioni, P. V. Eisenlohr, M. J. G. Pessoa, and I. V. da Silva, "Elucidating Adaptive Strategies From Leaf Anatomy: Do Amazonian Savannas Present Xeromorphic Characteristics?," *Flora* 226 (2017): 38–46, https://doi.org/10.1016/j.flora.2016.11.004.

38. S. M. Gomes, N. S. D. N. Somavilla, K. M. Gomes-Bezerra, S. d. C. de Miranda, P. S. Carvalho, and D. Graciano-Ribeiro, "Anatomia foliar de espécies de Myrtaceae: contribuições à taxonomia e filogenia," *Acta Botânica Brasílica* 23 (2009): 224–238, https://doi.org/10.1590/S0102-33062009000100024.

39. A. Donato and B. Morretes, "Morfo-anatomia foliar de *Myrcia multiflora* (Lam.) DC," *Revista Brasileira de Plantas Medicinais* 13 (2011): 43–51, https://doi.org/10.1590/S1516-05722011000100007.

40. N. V. Pacheco-Silva and A. M. Donato, "Morpho-Anatomy of the Leaf of *Myrciaria Glomerata*," *Revista Brasileira de Farmacognosia* 26 (2016): 275–280, https://doi.org/10.1016/j.bjp.2015.12.002.

41. J. F. Richit, S. V. N. Díaz, L. F. P. Dick, and J. E. A. Mariath, "Neither Lysigenous nor Just Oil: Demystifying Myrtaceous Secretory Cavities," *American Journal of Botany* 110 (2023): e16248, https://doi.org/10.1002/ajb2.16248.

42. Ü. Niinemets, "Storage of Defense Metabolites in the Leaves of Myrtaceae: News of the Eggs in Different Baskets," *Tree Physiology* 38 (2018): 1445–1450, https://doi.org/10.1093/treephys/tpy115.

43. M. Cascaes, G. Guilhon, E. Andrade, M. Zoghbi, and L. Santos, "Constituents and Pharmacological Activities of *Myrcia* (Myrtaceae): A Review of an Aromatic and Medicinal Group of Plants," *International Journal of Molecular Sciences* 16 (2015): 23881–23904, https://doi.org/10.3390/ijms161023881.

44. A. Mithöfer and W. Boland, "Plant Defense Against Herbivores: Chemical Aspects," *Annual Review of Plant Biology* 63 (2012): 431–450, https://doi.org/10.1146/annurev-arplant-042110-103854.

45. R. d. C. d. O. Arruda and C. P. Victório, "Leaf Secretory Structure and Volatile Compounds of *Eugenia copacabanensis* Kiaersk. (Myrtaceae)," *Journal of Essential Oil Research* 23 (2011): 1–6, https://doi.org/10.1080/10412905.2011.9700472.

46. V. C. Kuster and F. H. A. Vale, "Leaf Histochemistry Analysis of Four Medicinal Species From Cerrado," *Revista Brasileira de Farmacognosia* 26 (2016): 673–678, https://doi.org/10.1016/j.bjp.2016.05.015.

47. C. V. dos Santos, A. P. Mallmann, A. G. Toledo, et al., "Composição Química, Atividade Antimicrobiana e Antioxidante do Óleo Essencial de Folhas *Myrcia palustris* DC. (MYRTACEAE)," *Research, Society and Development* 10 (2021): e20510313303, https://doi.org/10.33448/rsd-v10i3.13303.

48. J. F. Rocha, R. R. Pimentel, and S. R. Machado, "Estruturas Secretoras de Mucilagem em *Hibiscus pernambucensis* Arruda (Malvaceae): Distribuição, Caracterização morfoanatômica e histoquímica," *Acta Botânica Brasílica* 25 (2011): 751–763, https://doi.org/10.1590/S0102-33062011000400003.

49. S. Bhambhani, K. R. Kondhare, and A. P. Giri, "Diversity in Chemical Structures and Biological Properties of Plant Alkaloids," *Molecules* 26 (2021): 3374, https://doi.org/10.3390/molecules26113374.

50. M. Heinrich, J. Mah, and V. Amirkia, "Alkaloids Used as Medicines: Structural Phytochemistry Meets Biodiversity—An Update and Forward Look," *Molecules* 26 (2021): 1836, https://doi.org/10.3390/molecules26071836.

51. R. K. Sindhu, A. Goyal, J. Das, S. Choden, and P. Kumar, "Immunomodulatory Potential of Polysaccharides Derived From Plants and Microbes: A Narrative Review," *Carbohydrate Polymer Technologies and Applications* 2 (2021): 100044, https://doi.org/10.1016/j.carpta.2021.100044.

52. C. Hou, L. Chen, L. Yang, and X. Ji, "An Insight Into Anti-Inflammatory Effects of Natural Polysaccharides," *International Journal of Biological Macromolecules* 153 (2020): 248–255, https://doi.org/10.1016/j.ijbiomac.2020.02.315.

53. T. M. Souza-Moreira, R. R. D. Moreira, L. V. S. Sacramento, and R. C. L. R. Pietro, "Histochemical, Phytochemical and Biological Screening of *Plinia cauliflora* (DC.) Kausel, Myrtaceae, Leaves," *Revista Brasileira de Farmacognosia* 20 (2010): 48–53, https://doi.org/10.1590/S0102-695X2010000100011.

54. L. Pérez-Gómez, A. T. Pérez-Martínez, A. Matheeussen, et al., "Phytochemical Characterization and Antifungal Potential of Leaf Extracts of *Mosiera bullata*," *Natural Product Research* 38 (2024): 3301–3310, https://doi.org/10.1080/14786419.2023.2244132.

55. J. V. Pereira, I. A. Freires, A. R. Castilho, M. G. da Cunha, H. da S. Alves, and P. L. Rosalen, "Antifungal Potential of *Sideroxylon obtusifolium* and *Syzygium cumini* and Their Mode of Action Against *Candida albicans*," *Pharmaceutical Biology* 54 (2016): 2312–2319, https://doi.org/10.3109/13880209.2016.1155629.

56. G. D. Marena, L. Girotto, L. L. Saldanha, et al., "Hydroalcoholic Extract of *Myrcia bella* Loaded Into a Microemulsion System: A Study of Antifungal and Mutagenic Potential," *Planta Medica* 88 (2022): 405–415, https://doi.org/10.1055/a-1323-3622.

57. C. C. Saulle, V. Raman, A. V. G. Oliveira, et al., "Anatomy and Volatile Oil Chemistry of *Eucalyptus saligna* Cultivated in South Brazil," *Revista Brasileira de Farmacognosia* 28 (2018): 125–134, https://doi.org/10.1016/j.bjp.2018.03.001.

58. N. R. Johnson and M. J. Axtell, "Small RNA Warfare: Exploring Origins and Function of Trans-Species microRNAs From the Parasitic Plant Cuscuta," *Current Opinion in Plant Biology* 50 (2019): 76–81, https://doi.org/10.1016/j.pbi.2019.03.014.

59. M. V. Busi, D. F. Gomez-Casati, M. Martín, et al., "Starch Metabolism in Green Plants," in *Polysaccharides* (Springer International Publishing, 2014), 1–42, https://doi.org/10.1007/978-3-319-03751-6_78-1.

60. L. Mondello, *FFNSC 2: Flavors and Fragrances of Natural and Synthetic Compounds, Mass Spectral Database*, 2nd ed. (Wiley Online Library, 2011).

61. A. S. A. El-Gaber, A. N. G. El Gendy, A. Elkhateeb, I. A. Saleh, and H. R. El-Seedi, "Microwave Extraction of Essential Oil From *Anastatica hierochuntica* (L): Comparison With Conventional Hydro-Distillation and Steam Distillation," *Journal of Essential Oil-Bearing Plants* 21 (2018): 1003–1010, https://doi.org/10.1080/0972060X.2018.1504695.

62. L. A. Conde-Hernández, J. R. Espinosa-Victoria, A. Trejo, and J. Á. Guerrero-Beltrán, "CO 2 -Supercritical Extraction, Hydrodistillation and Steam Distillation of Essential Oil of Rosemary (*Rosmarinus officinalis*)," *Journal of Food Engineering* 200 (2017): 81–86, https://doi.org/10.1016/j.jfoodeng.2016.12.022.

63. L. Silva, S. Sarrazin, R. Oliveira, C. Suemitsu, J. Maia, and R. Mourão, "Composition and Antimicrobial Activity of Leaf Essential Oils of *Myrcia sylvatica* (G. Mey.) DC," *European Journal of Medicinal Plants* 13 (2016): 1–9, https://doi.org/10.9734/ejmp/2016/25494.

64. E. M. H. Saccol, I. Jerez-Cepa, G. M. Ourique, et al., "*Myrcia sylvatica* Essential Oil Mitigates Molecular, Biochemical and Physiological Alterations in *Rhamdia quelen* Under Different Stress Events Associated to Transport," *Research in Veterinary Science* 117 (2018): 150–160, https://doi.org/10.1016/j.rvsc.2017.12.009.

65. S. B. Nerilo, G. H. O. Rocha, C. Tomoike, et al., "Antifungal Properties and Inhibitory Effects Upon Aflatoxin Production by *Zingiber officinale* Essential Oil in *Aspergillus flavus*," *International Journal of Food Science and Technology* 51 (2016): 286–292, https://doi.org/10.1111/ijfs.12950.

66. L. C. Vasconcelos, T. T. Carrijo, A. N. Venancio, et al., "Phytochemical Screening and Phytocytotoxic Effects of the Tropical *Myrcia vittoriana* (Myrtaceae)," *Anais da Academia Brasileira de Ciências* 94 (2022): e20210820.

67. O. O. Ferreira, J. N. da Cruz, C. d. J. P. Franco, et al., "First Report on Yield and Chemical Composition of Essential Oil Extracted From *Myrcia eximia* DC (Myrtaceae) From the Brazilian Amazon," *Molecules* 25 (2020): 783, https://doi.org/10.3390/molecules25040783.

68. Z. A. A. Aziz, A. Ahmad, S. H. M. Setapar, et al., "Essential Oils: Extraction Techniques, Pharmaceutical and Therapeutic Potential – A Review," *Current Drug Metabolism* 19 (2018): 1100–1110, https://doi.org/10.2174/1389200219666180723144850.

69. D. W. Christianson, "Structural and Chemical Biology of Terpenoid Cyclases," *Chemical Reviews* 117 (2017): 11570–11648, https://doi.org/10.1021/acs.chemrev.7b00287.

70. Y. Yuan, M. Litzenburger, S. Cheng, et al., "Sesquiterpenoids Produced by Combining Two Sesquiterpene Cyclases With Promiscuous Myxobacterial CYP260B1," *ChemBioChem* 20 (2019): 677–682, https://doi.org/10.1002/cbic.201800670.

71. E. R. Lanier, T. B. Andersen, and B. Hamberger, "Plant Terpene Specialized Metabolism: Complex Networks or Simple Linear Pathways?," *Plant Journal* 114 (2023): 1178–1201, https://doi.org/10.1111/tpj.16177.

72. L. Tsigoriyna, C. Sango, and D. Batovska, "An Update on Microbial Biosynthesis of β-Caryophyllene, a Sesquiterpene With Multi-Pharmacological Properties," *Fermentation* 10 (2024): 60, https://doi.org/10.3390/fermentation10010060.

73. M.-M. Lo, Z. Benfodda, R. Molinié, and P. Meffre, "Volatile Organic Compounds Emitted by Flowers: Ecological Roles, Production by Plants, Extraction, and Identification," *Plants* 13 (2024): 417, https://doi.org/10.3390/plants13030417.

74. J. M. Nguta, J. M. Mbaria, D. W. Gakuya, P. K. Gathumbi, J. D. Kabasa, and S. G. Kiama, "Cytotoxicity of Antimalarial Plant Extracts From Kenyan Biodiversity to the Brine Shrimp, *Artemia salina* L. (Artemiidae)," *Drugs and Therapy Studies* 2 (2012): 12, https://doi.org/10.4081/dts.2012.e12.

75. L. J. Gatto, N. T. Fabri, A. M. de Souza, et al., "Chemical Composition, Phytotoxic Potential, Biological Activities and Antioxidant Properties of *Myrcia hatschbachii* D. Legrand Essential Oil," *Brazilian Journal of Pharmaceutical Sciences* 56 (2020): 1–9, https://doi.org/10.1590/s2175-97902019000318402.

76. A. Judžentienė and J. Būdienė, "Mugwort (*Artemisia vulgaris* L.) Essential Oils Rich in Germacrene D, and Their Toxic Activity," *Journal of Essential Oil Research* 33 (2021): 256–264, https://doi.org/10.1080/10412905.2020.1857854.

77. F. Conforti, F. Menichini, M. R. Loizzo, et al., "Antioxidant, α-Amylase Inhibitory and Brine-Shrimp Toxicity Studies on *Centaurea centaurium* L. Methanolic Root Extract," *Natural Product Research* 22 (2008): 1457–1466, https://doi.org/10.1080/14786410802098071.

78. M. Mahboubi, "*Zingiber officinale* Rosc. Essential Oil, a Review on Its Composition and Bioactivity," *Clinical Phytoscience* 5 (2019): 6, https://doi.org/10.1186/s40816-018-0097-4.

79. M. Amina, P. Alam, M. K. Parvez, et al., "Isolation and Validated HPTLC Analysis of Four Cytotoxic Compounds, Including a New Sesquiterpene From Aerial Parts of Plectranthus Cylindraceus," *Natural Product Research* 32 (2018): 804–809, https://doi.org/10.1080/14786419.2017.1363750.

80. X. Pang, B. Almaz, X.-J. Qi, et al., "Bioactivity of Essential Oil From *Atalantia buxifolia* Leaves and Its Major Sesquiterpenes Against Three Stored-Product Insects," *Journal of Essential Oil-Bearing Plants* 23 (2020): 38–50, https://doi.org/10.1080/0972060X.2020.1729245.

81. A. M. Abd-ElGawad, A. I. Elshamy, A. El-Nasser El Gendy, S. L. Al-Rowaily, and A. M. Assaeed, "Preponderance of Oxygenated Sesquiterpenes and Diterpenes in the Volatile Oil Constituents of *Lactuca serriola* L. Revealed Antioxidant and Allelopathic Activity," *Chemistry & Biodiversity* 16 (2019): e1900278, https://doi.org/10.1002/cbdv.201900278.

82. A. Assaeed, A. Elshamy, A. E. N. El Gendy, B. Dar, S. Al-Rowaily, and A. Abd-ElGawad, "Sesquiterpenes-Rich Essential Oil From Above Ground Parts of Pulicaria Somalensis Exhibited Antioxidant Activity and Allelopathic Effect Onweeds," *Agronomy* 10 (2020): 399, https://doi.org/10.3390/agronomy10030399.

83. O. O. Ferreira, C. d. J. P. Franco, E. L. P. Varela, et al., "Chemical Composition and Antioxidant Activity of Essential Oils From Leaves of Two Specimens of *Eugenia florida* DC," *Molecules* 26 (2021): 5848, https://doi.org/10.3390/molecules26195848.

84. M. C. S. Neta, C. Vittorazzi, A. C. Guimarães, et al., "Effects of β-Caryophyllene and *Murraya paniculata* Essential Oil in the Murine Hepatoma Cells and in the Bacteria and Fungi 24-h Time-Kill Curve Studies," *Pharmaceutical Biology* 55 (2017): 190–197, https://doi.org/10.1080/13880209.2016.1254251.

85. C. d. J. P. Franco, O. O. Ferreira, Â. A. B. de Moraes, et al., "Chemical Composition and Antioxidant Activity of Essential Oils From *Eugenia patrisii* Vahl, *E. punicifolia* (Kunth) DC., and Myrcia Tomentosa (Aubl.) DC., Leaf of Family Myrtaceae," *Molecules* 26 (2021): 3292, https://doi.org/10.3390/molecules26113292.

86. C. d. F. A. Nonato, C. J. Camilo, D. O. D. Leite, et al., "Comparative Analysis of Chemical Profiles and Antioxidant Activities of Essential Oils Obtained From Species of *Lippia* L. by Chemometrics," *Food Chemistry* 384 (2022): 132614, https://doi.org/10.1016/j.foodchem.2022.132614.

87. L. S. da Costa, O. O. Ferreira, L. G. N. Lobato, et al., "Exploring Phytochemistry, Antioxidant Capacity, and Biological Potential of Essential Oils Obtained From Euphorbiaceae Species," *Phytochemistry Reviews* 24 (2024): 4101–4124, https://doi.org/10.1007/s11101-024-10031-3.

88. J. Rumpf, R. Burger, and M. Schulze, "Statistical Evaluation of DPPH, ABTS, FRAP, and Folin-Ciocalteu Assays to Assess the Antioxidant Capacity of Lignins," *International Journal of Biological Macromolecules* 233 (2023): 123470, https://doi.org/10.1016/j.ijbiomac.2023.123470.

89. D. Aebisher, J. Cichonski, E. Szpyrka, S. Masjonis, and G. Chrzanowski, "Essential Oils of Seven Lamiaceae Plants and Their Antioxidant Capacity," *Molecules* 26 (2021): 3793, https://doi.org/10.3390/molecules26133793.

90. M. Parcheta, R. Świsłocka, S. Orzechowska, M. Akimowicz, R. Choińska, and W. Lewandowski, "Recent Developments in Effective Antioxidants: The Structure and Antioxidant Properties," *Materials (Basel)* 14 (2021): 1–24, https://doi.org/10.3390/ma14081984.

91. K. Kut, B. Cieniek, I. Stefaniuk, G. Bartosz, and I. Sadowska-Bartosz, "A Modification of the ABTS• Decolorization Method and an Insight Into Its Mechanism," *PRO* 10 (2022): 1288, https://doi.org/10.3390/pr10071288.